CODEN:LUTEDX/(TEIE-5497)/1-95(2023)

Industrial Electrical Engineering and Automation

Investigating Sensor-based Condensation Detection in Network Cameras using Psychrometry

Emil Hermansson
Viktor Hansson

Division of Industrial Electrical Engineering and Automation
Faculty of Engineering, Lund University

Investigating Sensor-based Condensation Detection in Network Cameras using Psychrometry

Emil Hermansson & Viktor Hansson

June 2023

Academic supervisor: Gunnar Lindstedt
Examiner: Johan Björnstedt
Company supervisor: Albin Berggren

LUND
UNIVERSITY

Abstract

The presence of fog, or condensation, poses significant challenges in various fields, including surveillance cameras. The main issue is that fog obstructs the cameras view, essentially rendering the camera ineffective for surveillance. Currently, preventative measures such as heating the camera is a remedy at the cost of significantly increased power consumption. This master's thesis is aimed to enable smarter fog prevention by detecting when fog is present. This is achieved by exploring and testing several fog detection techniques from different industries to develop a prototype capable of detecting the presence of fog.

Four techniques: hygrometry, capacitance, resistance and infrared were initially investigated where hygrometry was decided as the most promising approach. This involves measuring temperature and humidity inside the camera in order to estimate the dew point temperature which is compared to the surface temperature where fog is prevalent. The temperature comparison represents a calculated indication of whether fog formation is theoretically possible. The results were encouraging, indicating promise that the concept could effectively detect fog.

The result and conclusion of this master's thesis is a developed proof of concept which is able to detect the presence of fogging in outdoor surveillance cameras. The solution consumes an insignificant amount of energy compared to the potential energy savings from detecting fog, demonstrates a potential to be reliable and finally, holds significant promise as an effective detection method.

Acknowledgements

The successful completion of this master's thesis would not have been feasible without the guidance, support, and expertise of numerous individuals to whom we owe a great debt of gratitude.
From the Division of Industrial Electrical Engineering and Automation at LTH, we express our sincere appreciation to both our supervisor Gunnar Lindstedt and our examiner Johan Björnstedt. Besides invaluable support during our master's thesis journey, both Gunnar and Johan have provided us with useful knowledge about electrical engineering and automation in our previous courses at the Lund Faculty of Engineering.

There are a few people at the company who we like to direct an extra thanks to. Firstly, We would like to express our heartfelt thanks to our supervisor, Albin Berggren, for his patient guidance, uplifting spirit and invaluable insights which filled our experience at the company with a sense of enjoyment and gratification. Additionally, we would like to thank Niclas Hörnquist from the Hardware quality assurance department for sharing knowledge and providing valuable insights from previous works in the field. His willingness to always find time to assist us was truly commendable.

Lastly, we want to express our gratitude to our peers for their camaraderie and moral support, which made this journey a memorable and enriching experience.

Contents

List of Figures

Chapter 1

Introduction

This chapter provides an introduction to the master's thesis project. It begins by detailing the need for a solution to detect fogging and frost while highlighting the associated problems and industry implications. The chapter also includes scope, goal, limitations, division of labor, abbreviations and an outline of this report.

1.1 Project description

This Master's thesis has been conducted in collaboration with a commercial camera company. The subject of this master thesis was proposed in order to find and prototype a solution to detect the presence of fogging and frost from condensation on the protective glass/plastic cover (referred to as the glass, cover or dome in this report) on outdoor network cameras. Initially, the scope also included finding methods of removing the fog and frost but this became disregarded due to being beyond the time constraints of the thesis work.

It is important to note that during the course of this study, the project owners at the collaborating company indicated that the use of external sensors would not be feasible for their cameras, primarily due to concerns about maintaining water resistance. This presented a unique challenge regarding frost detection since frost predominantly forms on the exterior of the camera, making its detection inherently complex. This heavily limited the design options for the frost detection solution.

Furthermore, the cameras which have internal heating elements to remove frost are already designed and required to operate at full power at temperatures significantly higher than those at which frost tends to form. Consequently, the detection of frost, though valuable, is somewhat mitigated by the cameras existing heat regulation system.

As a result of these considerations, the primary focus of this study shifted towards the detection of fog, with only secondary attention given to frost detection. This pivot was primarily driven by

the increased complexity of external frost detection and the preexisting camera counter measures for frost. However, some insights regarding frost detection are still included since fog and frost can be related and in order to provide a more comprehensive understanding of the phenomenon.

The need to detect fog and frost, primarily on surfaces, is present in several applications. Some fields where studies has been conducted are agriculture, white goods, energy and the automobile industry. Within these areas, the consequential issues caused by fog and frost vary, but some examples are inefficiencies, safety risks, loss of profits, and loss of visibility. Furthermore, just as the issues are varying, so are the implemented and proposed solutions, and as in many engineering applications, one solution created for a curtain application may be useful in other applications as well.

A common problem with outdoor installed cameras is the risk of the outermost transparent material getting covered by either fog or frost. This is often a visual obstruction that can result in greatly reduced visibility and render the camera incapable of producing any useful result for multiple days or weeks according to internal sources at the company. As the main purpose for many cameras is surveillance, this issue is not only a nuisance but a substantial consequence resulting in high maintenance costs, increased security risks, lost productivity, reduced customer satisfaction and regulatory/legal compliance issues in industries where a functioning surveillance system is required. However, accurately detecting fogging and frost presents a considerable challenge. For instance, simply activating a heating element at a temperature threshold can remove the mentioned issues, but at a high energy consumption and no guarantee that the heating is enabled only at useful times. Therefore is not reliable nor efficient in cost or power consumption.

Another problem is that there are no implemented methods to distinguish between fog and frost from each other. Therefore, the current solution is to have a wiper or to use a heater, but these methods require an excess of power or regular maintenance and may be inefficient if fog is detected as frost or vice versa. By implementing a sensor suite, it could be possible to verify if the camera lens is covered by fog or frost and afterward activate a suitable removal method.

1.2 Scope and goal

The main goal of this project was to develop a proof of concept for an energy-efficient and reliable solution for detecting the presence of fog and frost from the protective glass cover on outdoor surveillance cameras. The solution was not required to be immaculate since the primary focus is to demonstrate the working principles. This allowed for a broader range of solutions and flexibility in meeting certain criteria, as long as the issues could reasonably be addressed in future work.

The criteria used during this master thesis are, in order of significance: reduced power demand, reduced energy consumption, reliability, low cost, and space compatibility. The main criterion is

reduced power demand since the issues with fog and frost could easily be solved today if power consumption was not a limiting factor. However, many network cameras are powered trough *power over ethernet* (PoE) and therefore has a limited power supply, meaning the power budget is strictly limited and any power savings are in high demand in order to allow other features to draw power.

The second criterion, reduced energy consumption is similar to the first with one difference; to reduce the long term average energy consumption instead of reducing maximum power usage, such as when a heater is activated in the camera. This would lower energy costs and enable longer activation time during battery powered operation.

Regarding the remaining criteria, low cost and small size are both valuable but reliability is paramount in order to maintain the high quality of the products. Also, the solution should be small enough to feasibly be able to fit within the products through size optimizations and cost efficient enough to feasibly be able to be implemented in production through component optimizations.

To achieve the goals, various methods for detecting fog, and secondly frost, or detecting properties closely related to fog formation was investigated, tested, interpreted, evaluated and adjusted. For quality assurance, these steps were conducted as an iterative process and strive to mimic the real world as closely as possible, given the budget and equipment available. Throughout this project, consultation from experts provided by the company and Lund University will be used as much as possible.

1.3 Division of labor

This master's thesis was equally divided between the authors Emil Hermansson and Viktor Hansson. Occasionally, the authors worked on independent tasks in order to be efficient, such as one person performing hardware assembly while the other writes code. However, recurring tasks were alternated as to allow both authors to gain equal experience with every task.

1.4 Limitations

The project was limited in time and therefore some limits have been set in order to increase the likelihood of success. The following criteria were set up at the beginning of the project:

- The scope of this project is not to design a final product that will go into production but rather to create a prototype as a proof of concept. Furthermore, The project will focus on detecting fog and frost by reading and interpreting electrical values from a sensor suite rather than using image analysis or data from the camera image sensor.
- All possible solutions to the problem cannot be studied in great detail. Therefore, the study will start broad to encompass a wide array of solutions in order to limit them down to the

most suitable method rather quickly. This is in order to ensure a final prototype can be constructed within the time limit.

- A prototype that is able to function seamlessly with multiple existing products would be advantageous for the company. However, due to time constraints, it may not be possible to conduct extensive testing on multiple products, which may result in the prototype being restricted to a limited number of products.

Initially, the scope of this master's thesis was to detect, distinguish, and remove fog and frost. However, given the time constraints of the project, it became evident that this range of investigation was overly ambitious. As a result, the scope was refined to concentrate solely on the detection of fog and secondly frost, depending on available time. Despite this adjustment, some progress and observations were made regarding disguising and removal, which is incorporated into the report. The primary emphasis, however, is to present discoveries in fog detection.

1.5 Acronyms and abbreviations

ADC	Analog-to-digital converter
DPT	Dew point temperature
DUT	Device under test
GUI	Graphical user interface
HVAC	Heating, ventilation, and air conditioning
IC	Integrated circuit
MCU	Microcontroller unit
MUX	Multiplexer
PCB	Printed circuit board
PoE	Power over ethernet
RH	Relative humidity

1.6 Outline

This report consists of six chapters as described below:

- **Chapter 1 - Introduction**: sets the stage by providing the context, problem statement, scope, and goals of the thesis.
- **Chapter 2 - Background**: presents an overview of relevant theory and introduces proposed detection methods.
- **Chapter 3 - Testing and Validation**: discusses the experimental procedures, testing methods, and validation techniques employed in the study.
- **Chapter 4 - Method**: elaborates on the specific methodologies adopted for fog and frost detection, including the design and implementation of the proposed solution.

- **Chapter 5 - Results**: illustrates the outcomes of the study, presenting the data collected and its analysis.
- **Chapter 6 - Discussion**: provides an interpretation of the results, discusses the implications of the findings, and suggests avenues for future work.

Chapter 2

Background

This chapter delves into the complexities of fog and frost detection, with a focus on the underlying processes and the techniques used for their detection. The discussion also encompasses insights from other industries such as automotive and refrigeration, where fog and frost detection are crucial for both safety and performance. The physical properties of the company's cameras, particularly in relation to how they influence fog formation, are also explored. The chapter concludes with an overview of several detection methods, providing a clear understanding of their functionality, advantages, and limitations.

2.1 The properties of the camera

The camera used for testing was used as a baseline to perform tests. The camera has pan, tilt & zoom (PTZ) capabilities, meaning the image sensor and optics can be moved through a graphical user interface, it is relatively large and features a restive heating element, three fans and plenty of excess interior space which, for this study, could be utilized to place sensors.

The camera operates using power over ethernet (PoE), facilitated by a midspan PoE injector. This setup permits both power supply and data communication through a single ethernet cable, which is connected to a midspan that in turn is connected to a mains outlet and a computer. This arrangement simplifies cable management and reduces power losses for customers since low voltage data is allowed to travel longer distances and the higher voltage power source is located closer to the product. However, it also limits flexibility in adjusting maximum power consumption due to the plug-and-play nature of PoE, which offers a fixed maximum power draw, in this instance, 60 watts. This implies that any increase in power consumption beyond the designated PoE class limit would necessitate substantial modifications to the customers' infrastructure and is one of the reasons why power efficiency is of significance in this master's thesis project.

2.2 Psychrometry

Psychrometry is the study of thermodynamic and physical properties of gas-liquid mixtures. This field of study is, among other things, able to generate useful predictions by considering experimentally gathered data on parameters such as relative and absolute humidity, wet bulb and dry bulb temperatures, dew point et cetera. The usefulness of psychrometry has proven to be crucial in multiple applications, particularly in industries where air, temperature, and vapor influences the process, such as the food processing industry [1] and the HVAC industry (Heating, ventilation, and air conditioning) [7].

Psychrometry has been a significant tool in this study, specifically for understanding the conditions behind when condensation forms. The psychrometric chart, as seen in figure 2.1, is a practical method to visualize the psychrometric conditions for air-vapor mixes. It includes seven properties that include:

- Absolute humidity (also known as humidity ratio)
- Dew point temperature
- Dry bulb temperature
- Enthalpy
- Relative humidity
- Specific volume
- Wet bulb temperature

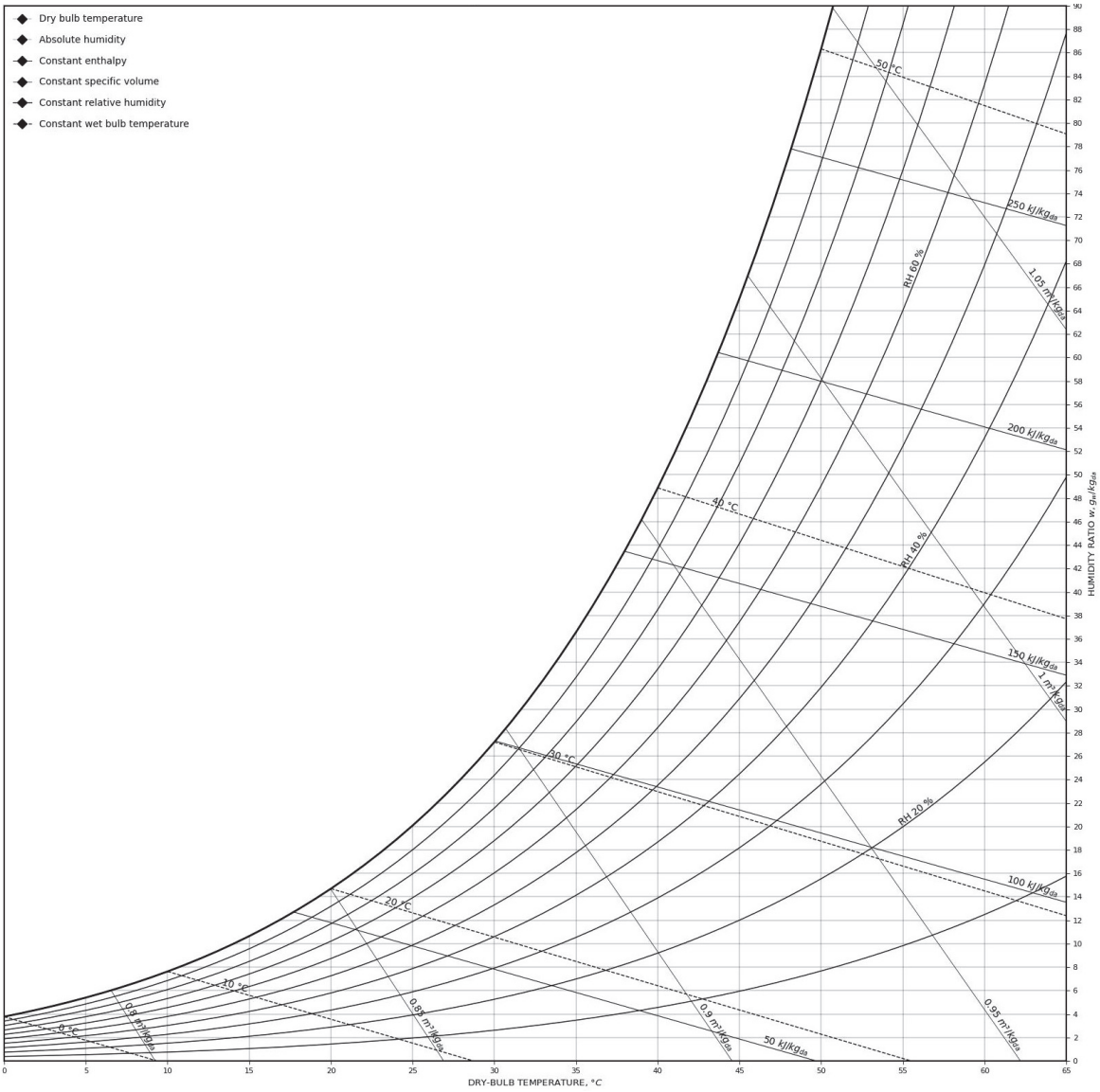

Figure 2.1: Example of a psychrometry chart. The horizontal axis displays dry bulb temperature and the vertical axis displays absolute humidity.

Figure 2.2 illustrates how the parameters are drawn and should be interpreted in a psychrometric chart. To fix the psychrometric state or, identify a specific point on the graph requires two measured parameters. Once these parameters are identified, the remaining characteristics can be inferred from the chart. However, it is important to note that a psychrometric chart is not a highly precise method for determining the state of the air, as it is visual and can be challenging to identify exact values. Nevertheless, the chart provides a visual representation of the experimentally gathered formulas behind air's psychrometric state, facilitating an easier understanding and visualization of changes in psychrometric conditions. [9].

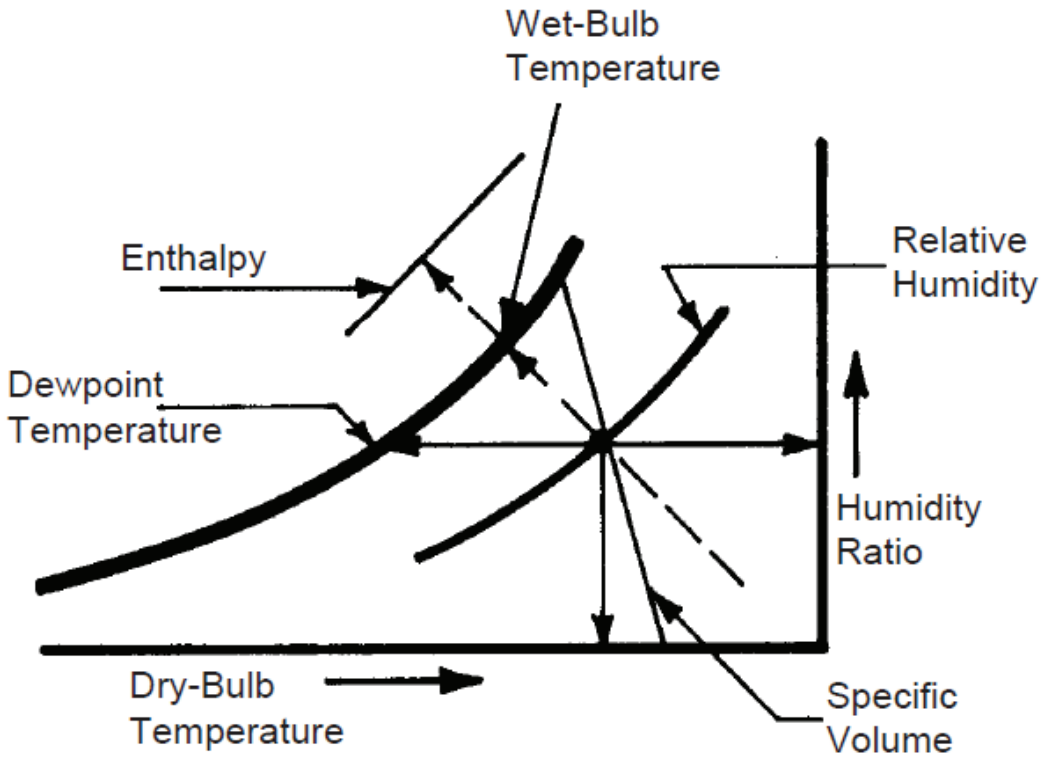

Figure 2.2: Illustration of the psychrometry chart properties [9]

The three key parameters for detecting fog and frost on a surface include dry bulb temperature, relative humidity, and dew point temperature. The dry bulb temperature is the temperature measured by a standard thermometer. The relative humidity is expressed as a percentage and relates the amount of moisture in the air compared to the maximum amount of moisture the air could hold at that temperature. The dew point temperature (DPT) is a temperature where saturation will occur if the air is cooled to the DPT, leading to over-saturation and therefore condensation. Understanding these three parameters is critical as they directly influence the conditions under which fog and, potentially, frost form. Since the wet bulb temperature, enthalpy and specific volume will not be used in the analysis in this thesis, they will not be plotted in the psychrometric charts. Hence the only parameters that will be included are dew point temperature, dry bulb temperature, relative humidity and absolute humidity. This simplifies the psychrometric charts which makes it simpler to read, an example of a simplified psychrometric chart can be seen in figure 2.3.

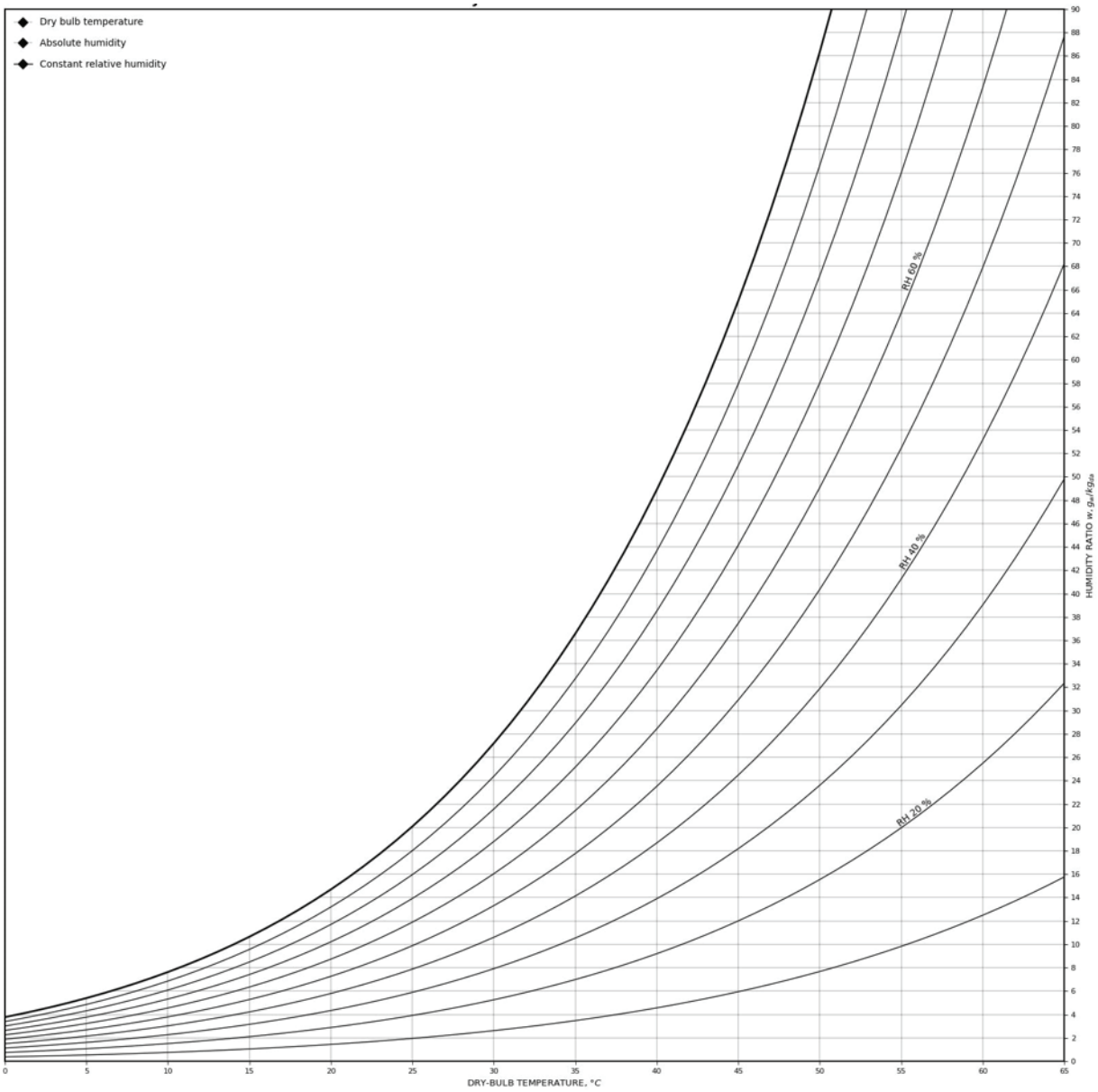

Figure 2.3: Simplified Psychrometric chart.

Knowledge of the current and historical state of the system, thus knowledge of the remaining parameters, does in theory determine whether conditions for condensate to appear are met or not. This particular example could be as follows, finding the intersection where the relative humidity and dry bulb temperature meet will pinpoint the state of the system. From there, the dew point temperature can be estimated and conclusively if any surface in the system is below the dew point, that surface would be prone to gather condensate. This explanation is visually illustrated in figure 2.4. The intersection is found by drawing a horizontal line from the current state of the air to the saturation line, illustrated with the dotted red line in the figure. At the saturation line, the dew point temperature is determined by drawing a vertical line, illustrated with the purple line in the

figure. The dry bulb temperature value at the vertical line is the current dew point temperature. If the glass temperature is lower than the glass temperature or in other words left of the purple line, condensation will occur.

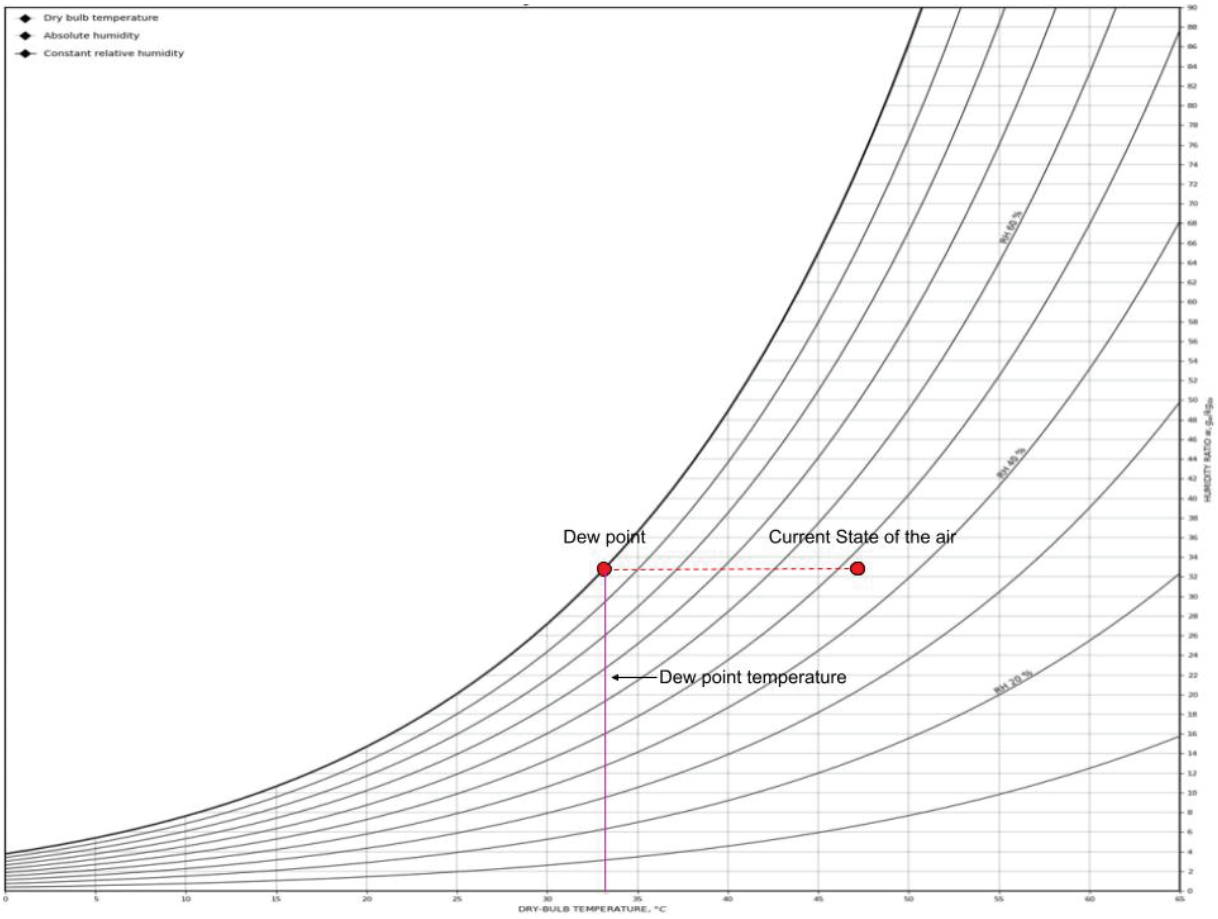

Figure 2.4: The dew point temperature of the air.

Another, and more realistic, method to estimate the dew point is through mathematical formulas. There are several formulas available to calculate the dew point given the air's relative humidity and temperature. However, in this project, the Magnus formula has been used, see equation 2.1 in section 2.10.1.

However, theoretical estimations versus actuality can cause issues in accuracy. It is nearly impossible to measure a real-world state accurately and guarantees can not be made. Regardless, baseline values and thresholds with an account for error can most certainly be of value. This is, for one reason, because it enables automated sensor readings that can calculate a probability of the presence or absence of visually impairing condensation which is the approach taken in this study.

2.3 Fog

Fogging is the process where water transitions from its gaseous to liquid state. This occurs when air with moisture cools below its dew point, typically upon contact with a cooler surface. As warm and moist air cools its relative humidity increases. Once it surpasses the dew point, the air is fully saturated and can not hold any more water. Water is released at this point from the air by condensing on the cooler surface. If the cooling continues, even more water will condense which can result in a decrease in the air's absolute humidity [10].

The definition of fog has a broad definition that includes more than what it is being referred to in this paper, a clarification of the definition of fog in this paper is: Fogging, fog or condensation in this report solemnly refers to the phenomenon when water condenses on a surface and forms fog unless specifically specified otherwise.

Fog formation is a complex phenomenon that is dependent on several parameters. However, since fog will not form unless the glass temperature is below the dew point temperature many of the problems can be simplified into two conditions:

- The humidity of the air, inside the system, is too high.
- The glass temperature is too low.

To exemplify a few common scenarios where fog is likely to form in this study, it will be compared with a few scenarios in which fogging usually occurs on the windshield of a car. The Article *"Clear Vision" Automatic Windshield Defogging System* [23] presents the following concrete cases of scenarios where fog can form on the windshield of a car:

1. When moisture is trapped inside the car after operation and the external temperature drops.
2. In tropical environments when the humidity approaches 100 % relative humidity.
3. Sudden temperature drop of the windshield that is caused by heavy rain during warm days.
4. The AC expels a significant increase in vapor moisture into the inlet air when starting the car if it has recently been used.
5. From a steady vapor stream generated by the passengers when driving in cold climates.
6. When a Passenger carries/introduces excess water into a cold car. This could be for example from having wet hair after a shower.

These cases illustrate the point that either the humidity inside the system is too high or the glass temperature is too low. Both of these criteria are derived from that the glass temperature has to be lower than the dew point temperature in order for the fog to form. Furthermore, Since these scenarios are described when fog is formed in a car and not a camera, the relevance of them forming

in a camera will therefore be discussed.

Scenario 1 due to the heat generated from the electrical circuits inside the camera, most parts of the cameras are supposedly warmer than the environment. So when the environment rapidly cools down it is likely that the moisture trapped inside condenses on the chilled surfaces that are thermally conductive and bridge to the outside environment.
Scenario 2 could have similar consequences in cameras as it does in cars. In such climates, the air is often near saturation point, meaning that even a minor temperature variation between the camera surface and the surrounding air can trigger condensation.
Scenario 3 is also likely to happen but is more dependent on the camera's orientation. Depending on how the camera is mounted, rain is more or less likely to hit the glass cover. However, if rain falls directly on the camera cover, it could be similar to a car windshield being cooled below the DPT of the air inside.
Scenario 4 has fewer similarities to a camera, yet parallels can be drawn. For instance, when a camera is activated it is also susceptible to fogging. This can occur if any trapped moisture inside the camera evaporates too quickly during start-up, leading to air saturation and subsequent condensation.
Scenario 5 passengers generating vapor can be compared to hygroscopic (water absorbing) materials in the camera which are prone to retain water and can expel moisture and cause saturation inside the camera, see section 2.8.
Scenario 6 is less likely to occur since the cameras have a high water and dustproof standard (IP-rating), which means that no water in liquid form can travel inside during normal operating conditions.

2.4 Frost

Frost is characterized by the solidification of water vapor or liquid on surfaces into ice crystals and is a surface phenomenon that occurs primarily in environments with high relative humidity. Its formation depends on a variety of external factors, including temperature, wind, and solar radiation, all of which interact with the surface structure of the object.

There are several types of frost, each with unique formation conditions and characteristics. Advection frost, forms when cold wind passes over warmer surfaces, drawing moisture that subsequently freezes on the surface. Window frost forms on glass surfaces when the outside temperature drops significantly which causes moisture from the warmer indoor air to freeze on the glass. Radiation frost occurs on clear, calm nights when objects lose heat by radiation and become colder than the surrounding air. Rime frost forms when supercooled water droplets in fog freeze upon contact with a surface [11].

The type of frost that forms can also be influenced by the surface structure. For instance, the

texture, porosity, and material of the surface can impact frost formation by affecting factors such as the surface's temperature and its ability to draw moisture.

According to information gathered from the quality assurance department at the company, frost forms primarily on the exterior surface of the glass. However, the occurrence of frost only appears during cold temperatures. Furthermore, frost is differing from fog since it depends heavily on external factors rather than controllable internal factors according to previous experience gathered by the company.

2.5 Heat transfer

The formation of both fog and frost is dependent on if the inner or outer glass cover temperature is lower than the dew point temperature of the inside or outside air. Therefore it is important to get an understanding of what the main factors are that affect the temperature of the surfaces the most. The inner and outer surface temperature of the glass cover will be affected by the heat transfer phenomenon of convection, conduction, and radiation. These heat transfer phenomena present themselves and are affected by different effects, both on the inside and outside of the camera. These effects include several meteorological conditions such as the inner and ambient temperature of the camera, the wind speeds outside, solar radiation level, and the presence of rain, and internal factors such as the heat produced by heaters and the camera system, the fan speeds and the properties of the materials in the system [8] [18].

The heat transfer conditions may vary a lot based on the installation location and orientation of the camera. For instance, depending on where the sunbeams hit the glass or what orientation the wind is blowing can change the temperature gradient over the glass drastically.

A schematic figure of how the temperature varies from the inside of the camera to the ambient could be seen in figure 2.5. The curve will differ in appearance depending on which heat transfer effects affect it and which of them is the dominant source of heat transfer. Furthermore, according to information gathered from the company, when the camera is on, heat will be generated from the internal electronics, causing the inner temperature to be higher than the ambient temperature. According to the first statement of the second law of thermal dynamics, heat flows spontaneously from hot to cold, the generated heat from the electrical components will be transferred from the inside of the camera, through the covering materials to the outside. When the heat generated by electrical components is equal to the heat being transferred out, the system is in steady state. During steady state, the temperature of the glass will be in between the ambient and the inside temperature. This is given that neither of them is undergoing a rapid change in temperature [18]. However when the ambient temperature drops, the heat transfer out of the camera will increase due to a bigger temperature gradient over the materials. This means that the heat stored inside the camera will start to decrease, and will continue to decrease until a new equilibrium state has

been reached. However, since the heat transfer rate is not infinite, the temperature is likely to drop continuously from the outside to the core. Meaning that the glass temperature is likely to decrease faster than the inside of the camera, hence will increase the risk of fog formation.

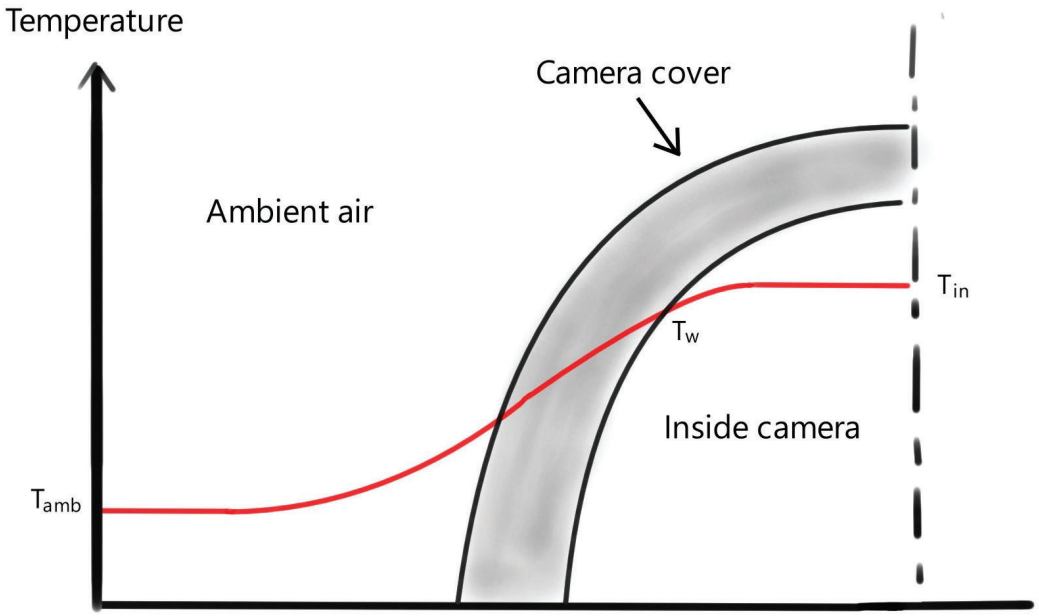

Figure 2.5: Schematic figure of how the temperature varies from ambient to the inside of the camera

2.6 Mass transfer of water within the camera

The camera can be analyzed as an open system. In an open system, the mass of material can be transferred both in and out of the system. When analyzing the mass transfer of moisture in the air, three main sources of transportation have been identified. These sources of mass transfer of moisture in the air are: Absorption into Hygroscopic materials, transportation through filters and potentially due to condensation. Additionally, there could occur some leakage through the seals, but this is assumed to be negligible for the sake of simplification.

2.7 Moisture transfer via filter vapor permeation

Outdoor camera enclosures are sealed for the purpose of being able to endure an outdoor climate. Specifically, the device used during testing has an IP66 rating, meaning it can withstand powerful

water jets from any direction without causing harm to the product. However, some moisture is able to penetrate into the product over time which is solved by integrating a hole with a breathable fabric membrane.

The vapor permeation caused by the membrane is not an area of focus in this study but understanding the implications caused by the membrane is still necessary. In simple terms, the membrane is assumed to be the main source for vapor to enter and exit the camera housing. Even if a small amount of moisture is transferred through other materials, this is considered negligible. The primary factor to take into account regarding the membrane is how it affects the speed of vapor transfer. In comparison to an open hole, the membrane causes a delay in the internal environment of the camera, resulting in a dampened system. This delay may contribute to the formation of fog. In particular, if the outside temperature and humidity levels remain high for an extended period of time and the temperature then suddenly drops, the inside temperature may fall more rapidly than the membrane can expel moisture. This will result in the air becoming saturated, leading to the occurrence of condensation.

2.8 Hygroscopic materials inside the device

The internal environment of the camera housing consists of many materials, which all have different properties regarding their ability to hold moisture or moisture retention capacities. This means some materials can retain moisture and if the humidity drops, these materials can act as a source of moisture for some time. Moisture retention is problematic in events where the temperature suddenly increases, such as when the sun shines directly on the camera housing or when the camera is initially powered on, these hygroscopic materials can act as a source of moisture and cause the formation of fog. This is due to the phenomenon of water vapor pressure, which causes moisture to move from areas of high concentration to areas of low concentration such as from a wet hygroscopic material to the surrounding air. As a result, it is essential to consider the role of these materials in the formation of fog and to develop strategies for minimizing their impact on the internal environment of the camera housing.

2.9 Cooling and dehumidification processes

Psychrometry is a key concept in this study and the topic is often used in HVAC systems. Therefore some terms in psychrometry may be out of place when utilized in this study, but regardless necessary to investigate. For instance, in an HVAC system, a common distinction is made between sensible cooling and latent cooling processes.

A sensible cooling process is when the temperature of the air is reduced meanwhile the absolute humidity is constant. In other words, the temperature of the air is dropped while the amount of

moisture in the air remains constant. Hence the result of a sensible cooling process is an increase in relative humidity and constant absolute humidity. [20]

A latent cooling process is when the water in the air starts to condense as a result of continuous cooling. This happens when the humidity of the air has reached the dew point and is continuously cooled down. Hence during a latent cooling process, the psychrometry of the air is aligned with the saturation/dew point line. [20]

When plotting the change between two states in a psychrometric chart, an arrow is drawn between the two states to indicate in what direction the process is moving in. Since the direction is otherwise unknown, and then it would be impossible to distinguish between a cooling and heating process in a psychrometric chart. However, this representation of the change of states in a psychrometric diagram is not totally accurate in regards to how the cooling process occurs in theory. Furthermore, the cooling process in figure 2.6 between states 1 and 2 includes both dehumidification and cooling of the air, since it decreases in both the x and y direction. Since state 2 has a lower temperature than the dew point temperature at state 1´, condensation is prone to happen. This means that the process both includes sensible and latent cooling. From a theoretical standpoint the cooling process will occur with the sensible cooling between state 1 and the intermediate state, 1' first, and then followed by a latent cooling between state 1' and state 2. [20]

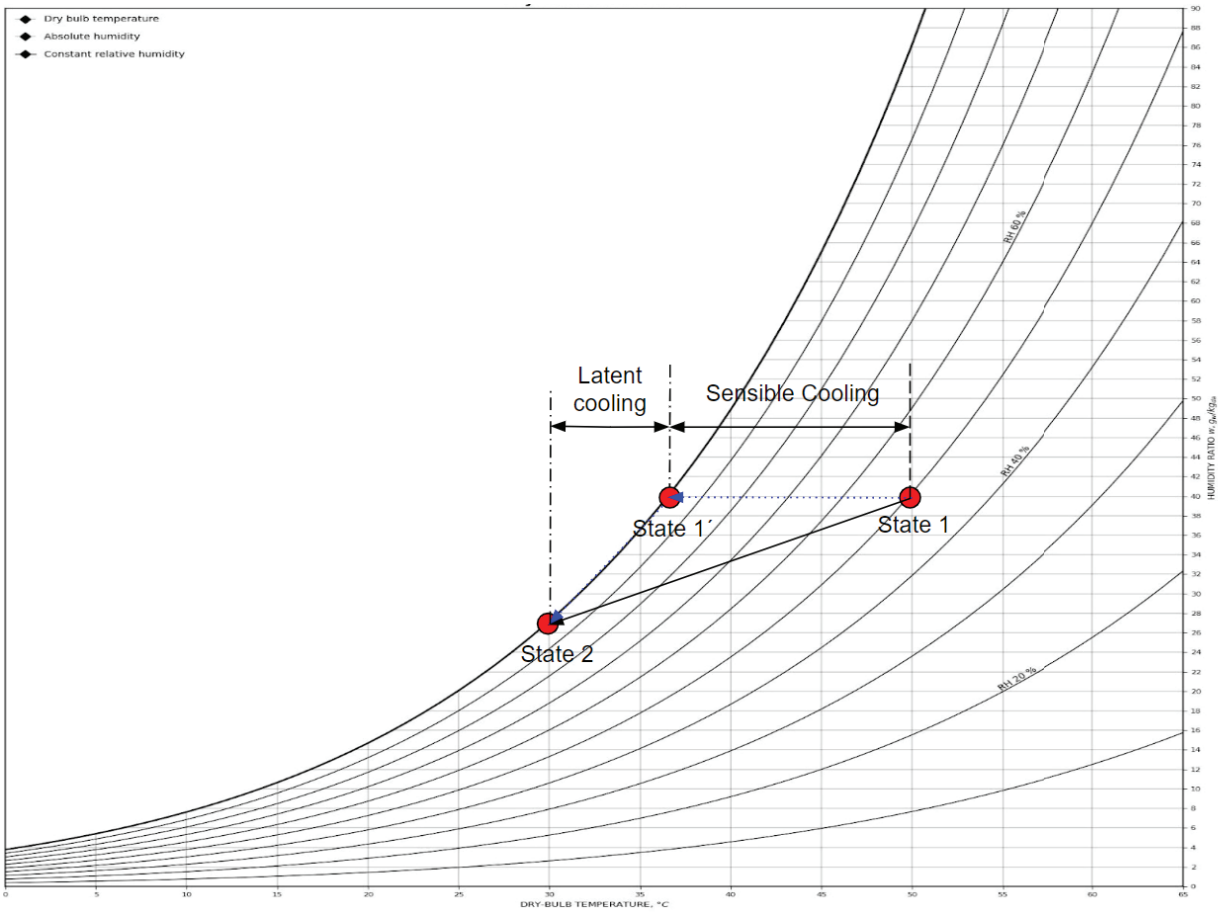

Figure 2.6: Cooling process of an HVAC system

2.10 Detection of fog and frost

There are several techniques for measuring fog and frost. For instance the article *Frost Measurement Methods for Demand Defrost Control Systems: A Review summarizes* [3] presents an overview of several techniques for measuring frost on an evaporator in a cooling system. The techniques presented in the mentioned article are Laser displacement gauge sensors, Photoelectric sensors, Fiber-optic sensors, Piezoelectric sensors, Capacitive sensors and Resistive sensors. Other techniques that have been found to either detect fog or/and frost are detecting Humidity and temperature sensing and IR-sensing. After having done a literature review of each technique, a few of them was picked out for further review and testing. The concepts that were picked for further investigation were:

- Detection of fog through psychrometry using detecting Humidity and temperature sensing
- Detecting fog and/or frost with a Resistive sensor
- Detecting fog and/or frost with a Capacitive sensor

- Detecting fog and/or frost with an IR sensor

2.10.1 Detection by utilizing psychrometry

One approach to detect fog on the inside of the camera is through a psychrometry approach. This could be done in different ways.

Estimating the window temperature through heat transfer estimation

One technique uses meteorological data, namely the wind speed, solar load, ambient temperature, humidity, temperature, and heat generation inside the camera to estimate the windshield temperature and cabin humidity. Through that, the DPT could be calculated and compared with the glass temperature. However, this technique has several disadvantages. Both that it requires the measurements of a lot of data, and that the data can be easily susceptible to measuring errors [22] causing a large error in the result. Furthermore to accurately account for all environmental conditions that could impact the system a multitude of parameters would need to be either measured or estimated. Such an undertaking would necessitate a complex climate system.

Comparing measured glass temperature with calculated dew point

Another method for detecting fog is to compare the glass temperature with the calculated dew point. This concept follows the following steps to evaluate the risk of fog. Firstly, Measure the glass temperature, the air temperature and relative humidity. Secondly calculate the air's dew point temperature with a suitable formula such as the Magnus formula 2.1, sourced from [15]. The Magnus Formula uses the relative humidity and temperature of the air to calculate the dew point of the air. The constants A and B are experimentally derived constants. Thirdly, Compare the calculated dew point with the glass temperature. In theory, if the glass temperature is lower than the dew point temperature, fog will form on the glass. However, if the glass temperature is higher than the dew point temperature, fog should not form. Hence the dew point temperature forms a threshold for when condensation forms [23]. This calculated difference, glass temperature subtracted by dew point temperature, will be referred to as *fog value* for the sake of simplicity in this study. The fog value will serve as an indicator for detection of fog. A positive fog value suggests a low likelihood of fog, while a zero or negative value indicates a probable fog occurrence.

$$T_{Dp} = \frac{B[ln(\frac{RH}{100}) + \frac{A \cdot T_{air}}{B+T_{air}}]}{A - ln(\frac{RH}{100}) - \frac{A \cdot T_{air}}{B+T_{air}}} \qquad A = 243.04 \quad B = 17.625 \tag{2.1}$$

A notable advantage of this method is its capability to provide comprehensive readings across the entire glass surface. The internal environment of the camera may not be uniform in temperature, thus strategic sensor placement becomes essential. Previous tests done by the company have shown that fogging can occur on only a portion of the glass, rather than the entirety of it. Thus, a sensor

such as a humidity sensor measures the conditions over more than just a small portion of the glass and is a great benefit.

Moreover, psychrometry as fog detection may be able to monitor more than just the surface of interest. Condensation forms on surfaces that are below the dew point temperature which may be multiple surfaces. In this case, the coldest surface is at the highest risk of condensation [16]. Therefore, a sensor on the glass could detect condensation forming elsewhere in the system if the glass temperature is below the dew point during a rapid decrease in humidity. This is because the system is sealed and water vapor is not able to suddenly exit the system. This means that the psychrometric approach has the benefit of being able to monitor the entire camera compared to other methods.

Fog detection utilizing psychrometry in other industries

This technique of detection has successfully been used in other applications, such as in buildings and cars. However, there are some differences such as cameras having internally large temperature gradients compared to a house or a car. This makes it more difficult to find a suitable measuring point in the camera that sufficiently represents the average temperature. Additionally, the smaller size of a camera compared to a house or a car entails space limitations and considerations about sensor placement such as not blocking visibility.

The report *A novel temperature–humidity–time defrosting control method based on a frosting map for air-source heat pumps* [24] shows that replacing the Temperature-Time frost controller with a Temperature-Humidity-Time frost controller resulted in a significant increase in accuracy and reduced the number of received false positives. This meant that better decisions could be automatically made when the system should be defrosted, which resulted in a better coefficient of performance, fewer misfires, and significant energy savings. Although this application significantly differs from the camera. Appealingly, by adding an extra hygrometer to the system, the need to warm the camera could be avoided in cases where the humidity is low enough. This would mean that the camera on average can hold a lower temperature, and thereby spend less energy on heating the camera, hence potentially achieving large savings of energy.

The article *Development and application of an integrated dew point and glass temperature sensor* [22] investigates how to implement humidity and temperature measurements in a car to detect fog. Furthermore, the article discusses where the sensors should be placed to achieve the best result. The report illustrates the importance of sensor placement and points out a couple of interesting considerations of what to consider when placing the fog detecting sensors in a car. Firstly, since there occur great temperature gradients, it is important to have the temperature sensor close to the humidity sensor in order to achieve an accurate measurement of the climate. Even though the temperature and relative humidity can vary significantly at different locations, the dew point should

remain relatively stable since the absolute humidity is approximately constant throughout the car cabin. Secondly, the results found that the ideal location to place the humidity and temperature sensor was near the rear window. This place had the best performance in detecting the risk of fog at the earliest 168 seconds before it was detected by the Infrared-sensor.

The article *System for early condensation detection and prevention in residential buildings* [16] investigates if it is possible to reduce the amount of fog on the inside walls of a building by implementing a humidity and temperature sensor system. The report's results emphasize that humidity has a more substantial impact on the dew point than temperature and therefore recommends using humidity ventilation instead of heating as a preventive measure. This is partly because heating can worsen condensation effects over time, given that warmer air can hold more moisture than cooler air. Furthermore, another subject that is discussed is where the sensors should or should not be placed. The authors suggest that a combined temperature and hygrometer sensor(a relative humidity sensor) should be placed in a location that is not affected by heaters or any moisture source since this would influence the psychrometric data and hence not be an accurate representation of the psychrometrics of the room. The article also states that the wall temperature sensor should be placed where condensation is the most likely to occur, this being the inside wall due to it being the coldest surface. These points were also confirmed by the results in the article *Development and application of an integrated dew point and glass temperature sensor* [22].

Miscellaneous takeaways from other industries

The risk of fog increases when relative humidity increases. The primary danger zone and area of interest when dealing with fog prevention is the range of 80-100 % relative humidity. Unfortunately, this is also the range where the humidity sensor has the biggest error. This is a concern since it makes it harder accurately measure the relative humidity in the area where it is of most importance. However the report *Development and application of an integrated dew point and glass temperature sensor* [22] studies how their result would be affected by having an error of 3 % and found out that the fog growth was still estimated well even with a 3 % error in relative humidity.

Another interesting observation that was found in the article *"Clear Vision" Automatic Windshield Defogging System* [23] was that during one of their tests for detecting fog, they found that after the fog removal heating had started, the relative humidity was observed to be 100% until all of the fog had evaporated. This is a highly interesting result since that could mean that it would not only be possible to detect when fog is formed but when all of it has evaporated as well.

Finally, the psychrometric movement of air will not instantaneously go from a binary state to another, it will rather approach the criteria of when fog is likely to form. Additionally, the fog formation itself will not happen instantaneously but will start to form slowly when these conditions

are met. This means that it can be used to predict fog rather than detect when fog has formed. The results in the report *Development and Application of an Integrated Dew Point and Glass Temperature Sensor* [22] showed that by using this technique fog could be predicted before it was detected by the IR sensors, meaning before the fog had actually formed. This information is interesting because as a result of predicting fog, the prevention techniques such as activating a heater could be started much earlier. This could potentially mean that significantly less energy has to be used since no fog has to be removed but rather merely prevented. Because the more amount of fog that is formed, the more energy is required to remove it.

2.10.2 Capacitive sensor

Capacitance refers to an ability to collect and store electrical charge, commonly through the electrical component known as a capacitor which has two plates close together with a dielectric material (insulator) as separation. However, capacitance does not only occur in designed capacitors but also whenever two conductors at different voltages are in close proximity, commonly referred to as parasitic capacitance. By utilizing this knowledge, it is possible to design moisture sensors based on the principles of capacitance.

In this study, capacitive sensing refers to electrically measuring a change in the dielectric constant in proximity to a capacitive sensor. This consists of a capacitive sensing circuit, abbreviated CSC, which measures a parameter such as voltage or time that can be converted into a capacitance value. The second part is the actual sensor, or electrode, which minimally is anything metal or conductive. The main considerations to be made when a design is chosen include sensitivity, accuracy, sensing direction, efficiency and complexity.

The main purpose of the CSC is to measure capacitance. The CSC can be designed to implement a variety of extra features to improve accuracy and efficiency but the main purpose is to measure the dielectric constant of a medium by measuring capacitance. For instance, this can be done with a simple RC circuit consisting of a known resistor and a known capacitor. The measurement electrodes can then be placed in parallel to the known capacitor, thus forming a pair with a joint measurable capacitance. The two electrodes form a variable capacitor with a default intermediate medium such as air and therefore a default capacitance. Any changes in the dielectric constant of the intermediate medium will thus change the capacitance in the RC circuit. In this example, moisture between the electrodes will increase the measured capacitance since water has a significantly higher dielectric constant than air (Approximately 80 for water and 1 for air) [17]. However, the goal is to detect moisture and not necessarily a large amount of moisture which requires a sufficiently sensitive CSC. Figure 2.7 shows a simplified illustration of a CSC where the resistor and capacitor are fixed and known, the variable capacitor is the electrodes, the voltmeter is any device capable of measuring voltage and the sinus alternating current source represents any component able to charge and discharge the circuit.

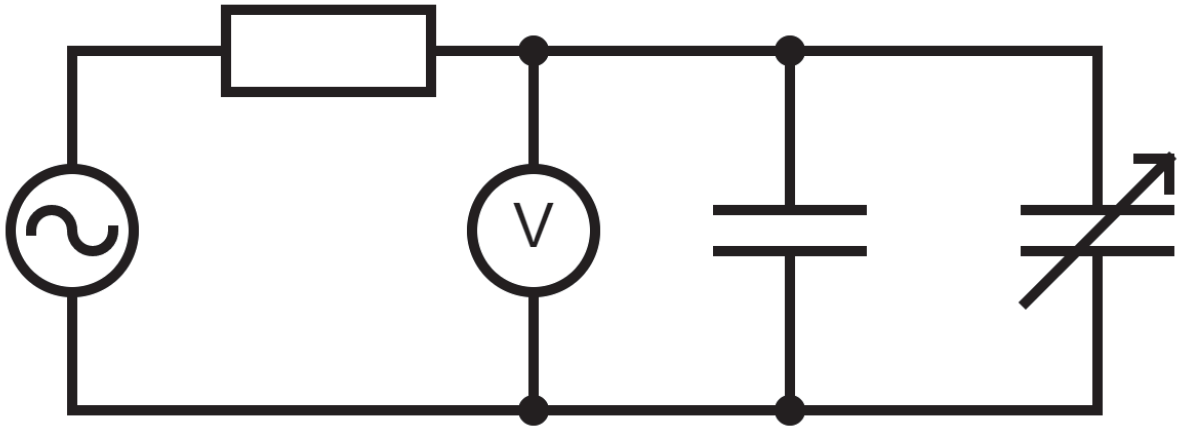

Figure 2.7: Simplified schematic of the main principles behind a capacitance sensing circuit based on a RC circuit.

Once a CSC has been designed, there are multiple methods of measuring capacitance. One common method which varies slightly depending on specific needs is to utilize the inherent behavior of charging and discharging a capacitor. Since the charging time of a capacitor is related to the capacitance value, calculating the capacitance can be done by measuring the time it takes to charge a capacitor through a series resistor. This can be done cost-efficient with low complexity, for example by using an MCU (microcontroller unit) and an ADC (analog-to-digital converter), where the MCU can time, control and read a digital representation of measured voltage from the ADC. However, frequent repeated charging and discharging can be an inefficient method regarding power consumption, but there are modifications that reduce power consumption at the cost of increased complexity. For instance, by adding circuitry and instead measure peak voltage it is possible to charge the capacitor for a shorter time period, such that the capacitor is not fully charged. From this, the measured peak voltage over the capacitor along with a known charging time can be used as an alternative method to calculate capacitance, but at a reduced power consumption for the CSC [19].

One additional thing to consider when designing the CSC is whether to use the self or mutual capacitance method. In both methods, two electrodes are connected to the CSC and placed close to each other in order to form a basic capacitor. In self capacitance, changes are measured with respect to ground meaning one active electrode forms one side of a capacitor and the other electrode is grounded. The emitted electric field travels between the active plate and the ground plate, and the measured capacitance is directly dependent on the dielectric constant of the intermediate medium. Mutual capacitance has a similar setup but one plate is regarded as the transmitter and the other as the receiver. When a disturbance with a high dielectric constant value, such as a human finger, gets into close proximity, the disturbance acts as a second, imaginary, receiver plate

which reduces the measured capacitance at the actual receiver plate [13].

The electrodes which are connected to the CSC and mounted in an area of interest can for instance be two parallel overlapping plates with a separator. However, some issues with this approach are that sensing occurs mainly in the area between the plates and the plates themselves may obstruct and interfere with the physical phenomenon that is being measured, such as measuring frost buildup. This can be reduced by using a mesh electrode instead of a solid plate. Alternatively, the interference can be further reduced by mounting the plates side by side on the same surface. Despite the plates being placed side by side instead of on top of each other, the configuration remains effective due to the nature of electric field propagation. Electric fields are inherently not confined to the area between capacitor plates; they can spread beyond the edges into the surrounding space. This phenomenon, known as the fringing field effect, allows the electric field to connect the plates even when they are arranged side by side. Additionally, since the fringing effect is beneficial, a sensor design that maximizes the fringing effect is desirable. One example of a design that achieves this is by interlacing the electrodes to maximize the total length of edges between the two electrodes, thus maximizing the area where the fringe effect occurs. This interlacing or comb-like structure is known as an interdigitated sensor array, see figure 2.8.

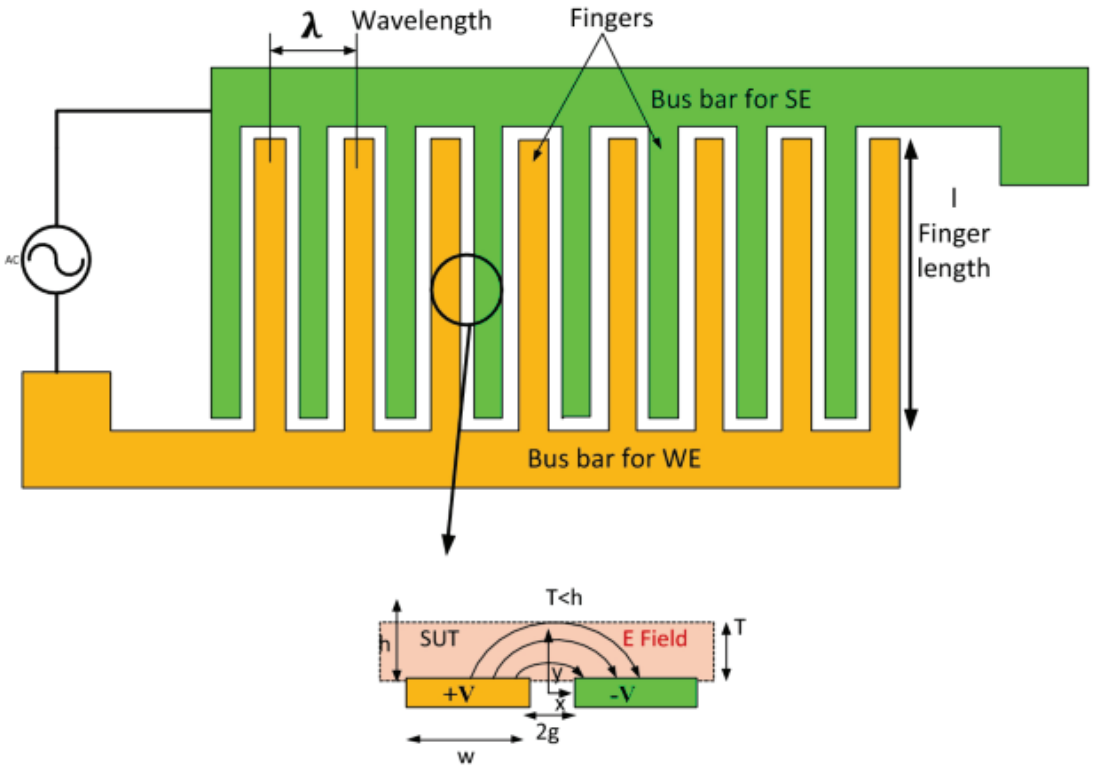

Figure 2.8: Schematic illustration of an interdigitated sensor array. The fringing field effect can be seen as the bent electric field lines in the bottom figure [14].

2.10.3 Resistive sensor

The resistive sensor technique is a low complexity and low cost technique for measuring fog and frost. Previous studies conducted on the cooling system of a refrigerator have used one of the following setups. In the setup shown in figure 2.9a the electric circuit consists of two ten kilo ohm resistors and a transistor to measure the change in resistance [12] meanwhile the other setup the electric circuit consisted of a voltage divider, connected to an analog to digital converter to interpret the signal as a 10-bit number, and thereby measure the voltage drop over the probe [4].

Both setups rely on similar techniques, that different materials and phases of the same material can have substantially different conductivity/resistivity. This means that depending on what material, either water (fog), air or frost, that is between the two probes/electrodes, the resistance will be substantially different which in turn will generate a significantly different voltage drop when a voltage is applied. When the two probes are separated by air there will be a large resistance in between them, resulting in a high voltage drop over the probe. However, when water forms a bridge in between the probes, as in figure 2.9b, the resistance between the two probes will drop significantly. Furthermore, frost has a distinguishable yet relatively close resistance to air. Hence

the formation of frost will cause the resistance to rise leading to a voltage drop between the probes. However, when frost formation occurs, the condensing of water will occur first followed by the water freezing. This will result in that when the formation of frost occurs there will first be a decrease in voltage from the formation of water and then when the water freezes the voltage will increase again.

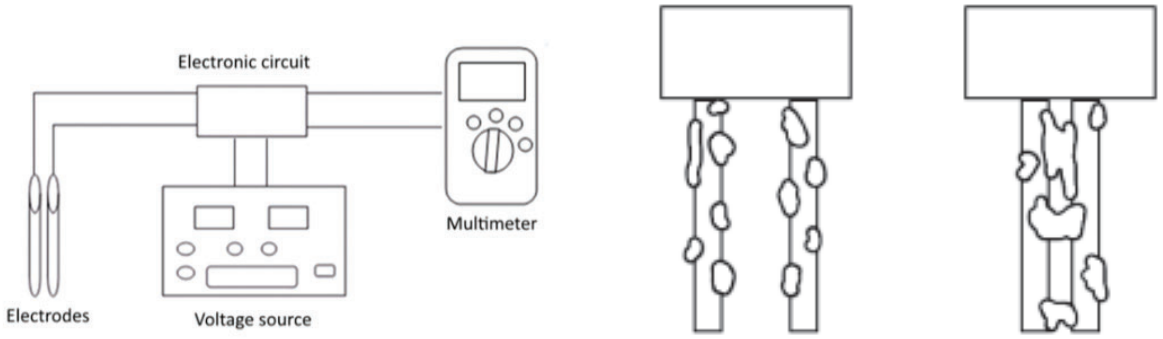

(a) (b)

Figure 2.9: (a) Sketch of experimental setup [12]. (b) Sketch of formation of water droplet to the left a water bridge to the right [4]

Several factors have been evaluated in order to achieve a satisfactory result, such as experimenting with the distance between the probes, different materials of the probes, what medium is best in between the probes and general sensor configurations.

One of the studies tested how the voltage of two probes varied when the distance was altered between three to eight millimeters in increments. The test was carried out with two different probe materials, zink, and copper, for three kinds of mediums in between the probes namely air, water and ice. The different materials showed similar results in voltage drop for the same medium and distance between the probes with only minor alterations. However, there was a big difference in voltage for different distances when the probes had water in between. There was also a small difference in voltage for ice as the internal medium for different distances. In extension, this also meant that it was possible to distinguish what material was currently between the probes, at distances less than five millimeters [4].

The presence of different materials between the probes was also tested with three kinds of material, namely Air, ceramic material, and fabricated medium. The materials were tested similarly to the technique mentioned above. The results showed that the fabricated medium, cotton in this test, had the best result. The air gap was also a good contender, but worse in accuracy than the fabricated medium. However, the ceramic medium was deemed not befitting for the application [6].

The probe setup which yielded the best result was also tested further. Several different probe

configurations were set up and tested, in order to detect as many frost cycles as possible. The prototypes, computer aided design (CAD) models and the results of the best air gap and cotton-wrapped sensors can be seen in figures 2.10a and 2.10b.

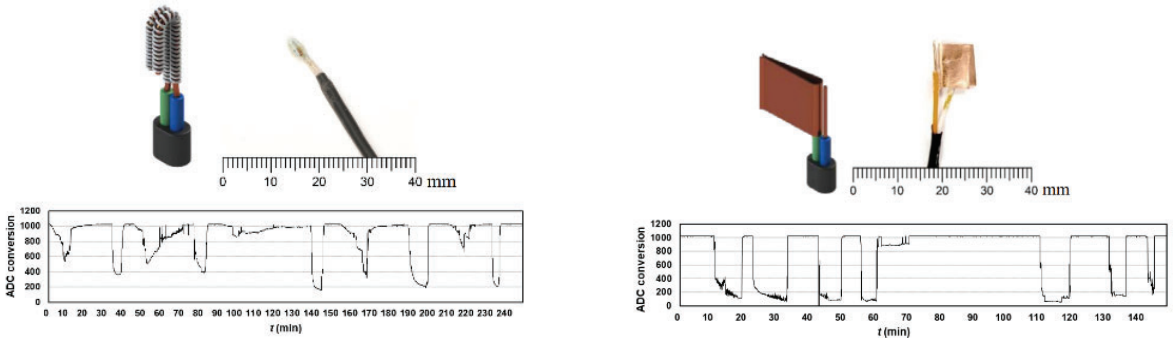

(a) (b)

Figure 2.10: (a) The best cuttonwraped-sensor and detection result [5]. (b) The best airgap sensor and detection result [5].

2.10.4 Infrared sensor

The infrared sensor can measure visibility obstructions such as fog or frost by transmitting and reading reflected infrared light. If the glass or plastic is unobstructed, most of the light will be transmitted through the transparent material. However if the material is covered by fog, frost or any other visual obstruction, some amount of the light will be reflected back. The reflective light will then be picked up and detected by the receiver, resulting in an increase in measured voltage [22].

An advantage of an infrared sensor is its potential reliability. This approach can detect fog but not predict it, meaning the benefits of prediction such as energy savings are lost, with the added benefit being more reliable by default. Additionally, the sensor should have high accuracy, capable of detecting the onset of fog or frost development before it becomes visible to the naked eye. However, the technique also presents some problematic limitations. The size of the sensor is relatively large, which could cause a problem when the sensor is placed inside a camera if the space is limited. Another disadvantage is that the sensor can only detect fog or frost formation locally. This results in that the fog or frost will not be detected by the sensor until it has started to form in front of the sensor which could happen rather late since the sensor typically should be mounted toward the edges of the glass. Another problem is that the sensor could also give a false positive value of fog and frost detection if there are other visually disturbing media such as dust or spiderwebs. Finally, even if the detection can happen at the early stages of fog or frost formation and has high reliability once the fog is formed a the sensor location, it would be beneficial to be able to predict the obstruction before it begins to form. [22].

Chapter 3

Initial tests

This chapter describes testing, validation and finally comparison of the four proposed methods of fog and frost detection. The test procedures and results for each method are presented and finally, one method is chosen to be investigated further.

3.1 Resistivity sensor

The setup for the resistivity sensor consisted of two metal wires separated by a small gap, on a flat glass cover. The resistance between the gap could then be measured when air compared to water bridged the two probes. The setup was tested both by simply measuring the resistance with an ohmmeter and by creating a voltage divider and measuring voltage. A reenactment of the simplest test setup can be seen in figure 3.1.

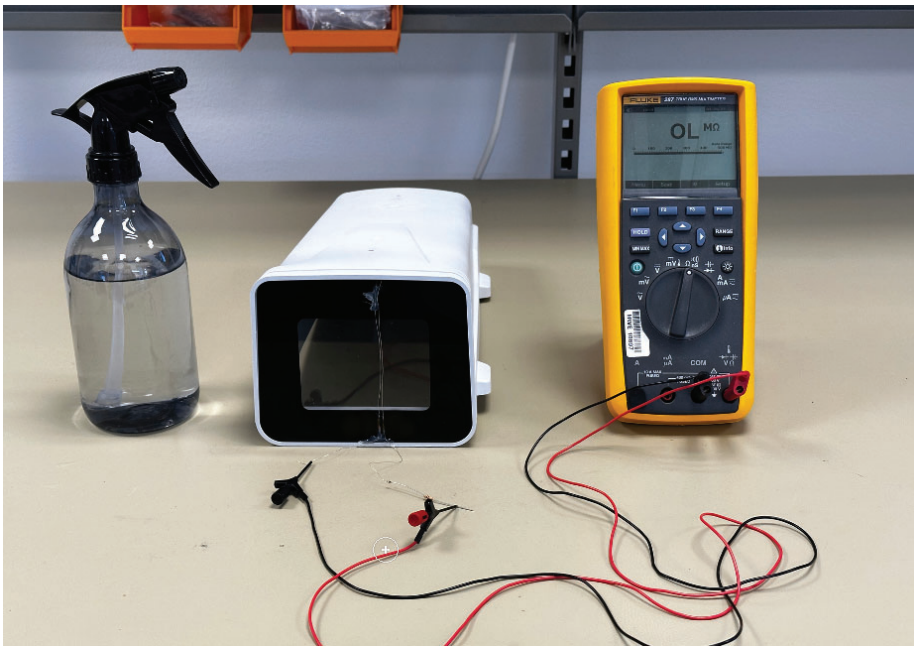

Figure 3.1: Test setup for the resistance concept.

In the first test, the probes were connected to a multimeter, and the resistance between the probes was measured. The electrical circuit of the test setup is found in figure 3.3a. The results of the test showed that the resistance between the probes when a water bridge was formed was around 1 $M\Omega$, see figure 3.2a, while the resistance for an air gap gave an overflow value ($> 500\ M\Omega$), see figure 3.1.

The second test involved soldering a 1 $M\Omega$ resistor in series to the probes and connected to a 12 volts power source. The voltage drop across the probes was measured both with water and air as a bridging medium. The corresponding electrical circuit diagram can be found in figure 3.3b. The voltage drop when water was present averaged around 6.4 volts, while it was approximately 12 volts in the presence of an air gap. The setup was tested with various known series resistors, up to 5 $G\Omega$ in order to detect the presence of water earlier. However, water was only ever detected once enough water was present to create a complete bridge that had a resistance of around 1 $M\Omega$. Hence the existence of fog was not enough to cause a resistance drop, as seen in figure 3.2b

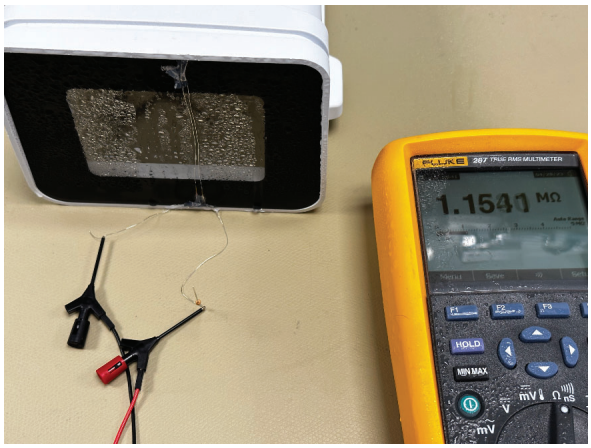

(a) Result from resistance measurements with water as a medium.

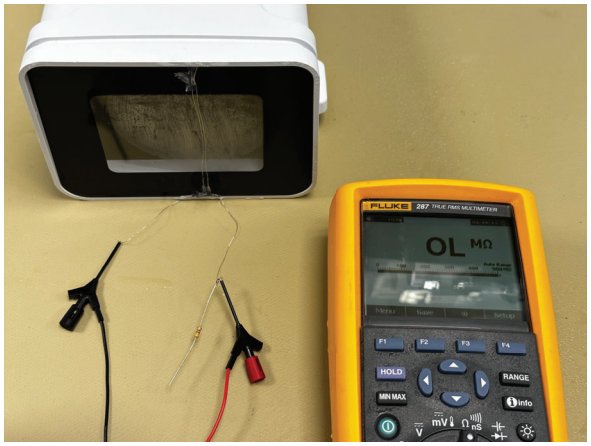

(b) Result from resistance measurements with fog as a medium.

Figure 3.2: Result from resistance measurement with different mediums.

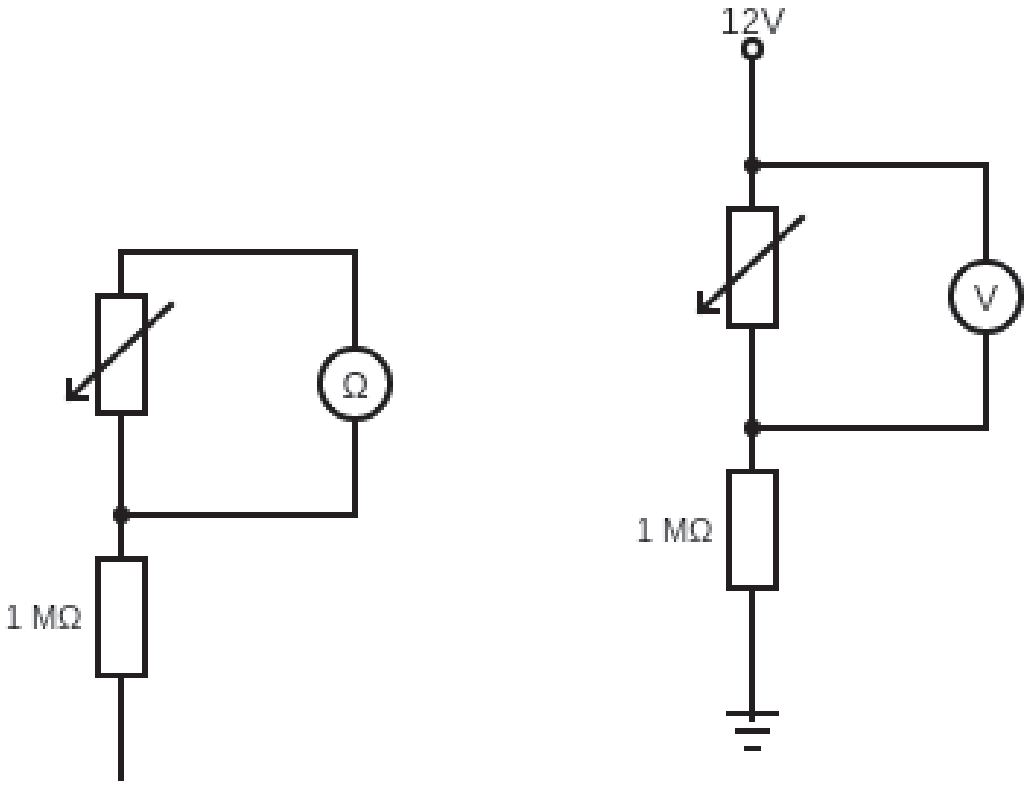

(a) Diagram of measuring resistance directly. Note, the 1 $M\Omega$ resistor is not affecting the readings.

(b) Diagram of the voltage divider setup.

Figure 3.3: Test setups of the resistance concept.

The tests were performed by applying water either by spraying a mist onto the probes or by using a wet paper towel. This was in order to test the best case scenario, where an abnormally large amount of water was applied. The results were somewhat successful at best but were unreliable and unpredictable.

Another issue with the resistance sensor is that it would only detect the existence of water locally and the sensor would preferably be placed in the corner of the camera cover, so as to not block the field of view. Hence the conclusion was that this technique is better suited for macro-applications when visibility is not an issue, such as the mentioned industries in subsection 2.10.1. As a disclaimer, the measuring technique of these tests was not the most accurate and could have been improved. For instance, the probes should be placed evenly with a small distance in between which was difficult to achieve as well as designing a more sensitive circuit. However, these tests were carried out as a quick proof of concept in order to validate whether further investigation could be justified.

3.2 Capacitive sensor

A widely used application for capacitive sensing is capacitive touch which is often used commercially as a means to interface with devices such as touch screens. As a result, there are multiple inexpensive integrated circuits and EVM's (evaluation modules) available for capacitive touch which, for this study, was used to initially evaluate captive sensing for fog detection.

The first EVM used in this st was the EV24Z38A from Microchip Technologies which, besides a capacitive sensing IC, has a built-in sensor, an active shield and multiple parameters to tweak such as sampling time, oversampling and sensitivity. However, the MTCH1010 IC which drives the EVM only has a binary output of touch or no touch, as opposed to an output with multiple values. This was known at the time of purchase and regarded as acceptable since the sensitivity could be adjusted as well as because the primary objective was only to evaluate whether condensate could be detected or not. By using the highest available sensitivity setting and constructing an external sensor attached to the glass of a camera, the EV24Z38A was able to detect water on the glass surface. However, the results were that water could be detected, but not with lower amounts of water, such as when a thin layer of fog covers the glass. Regardless, the tests were considered a success since they did in fact confirm the simpler hypothesis of being able to detect water droplets, even through the glass.

As a continuation of the EV24Z38A tests, a more accurate and able EVM was purchased in order to evaluate whether capacitive sensing could be used to detect lower amounts of condensate. The EVM used was the FDC1004EVM which is based on the FDC1004 capacitance-to-digital converter from Texas Instruments. The EVM features all necessary circuitry to support the FDC1004 such as reference capacitor, oscillator, sensor, active shield, I2C and USB interface and has a measurement resolution of 0.5 fF (femtofarad) according to the supplied datasheet from Sensorion [2]. After connecting the necessary I2C communication pins to an Arduino UNO microcontroller and writing a suitable communication script in C++, the output values could be plotted. Initial tests were performed by covering the sensor with a layer of plastic and using a spray bottle to apply a fine layer of mist on the sensor. The mist showed a slight but notable increase in measured capacitance which was deemed a satisfactory result. However, the observed increase was rather low and could potentially pose challenges for automated detection through software, especially considering the substantial noise present at these lower levels, thereby resulting in a low signal-to-noise ratio.
The preliminary testing showed one major advantage of the capacitance sensing approach which is detection through the glass where frost is the primary concern. Although frost was no longer within the primary scope of this study, the knowledge could prove useful in frost detection applications.

3.3 Humidity and temperature sensor

To determine the feasibility of fog detection using a combined temperature and humidity sensor, one such sensor was positioned within the camera cover for evaluation. The idea of the test was to see whether the hygrometer would measure a higher relative humidity if the fog was created on the inside of the glass cover. This was partly done to see the reliability of the sensor's measurements. To generate fog on the inside, a cup of boiling water was placed inside the camera cover, see figure 3.4. The humidity was then measured using an Arduino which is further described in subsection 4.1.1. The result was that the hygrometer measured a high relative humidity when fog formed. High humidity readings were also recorded even when the fog was far from the sensor. Additionally, the humidity readings remained high until most of the fog disappeared from passive evaporation into the air.

These initial tests were seen to have high potential. Knowing that the sensor reliably recorded a high value during the entire duration while the fog was present was positive and motivated further testing.

Figure 3.4: Test setup for testing of the hygrometer. The picture is taken during maximum fog presence.

Since it was crucial to use a sensor with high accuracy, a test was performed in order to validate the accuracy of the humidity sensor. The sensor was placed in a climate chamber with the relative humidity set to 95 % and the temperature set to 20° C. The difference in the measured humidity in the temperature chamber and the sensor was less than 2 percentage point. The accuracy was deemed satisfactory and on point according to the datasheet, especially considering that the accuracy is specified to be worse at higher humidity levels.

3.4 Infrared sensor

Infrared sensors or IR sensors, encompass a broad range of devices that detect and measure infrared radiation. This study focuses on active IR sensors, which emit and receive bounced IR light. Examples of such sensors include IR proximity sensors and IR motion detector sensors. For a more detailed description, refer to subsection 2.10.4.

During the course of this study, the purchase and testing of IR sensors were by chance the last method to evaluate. As a result, when it was determined through interviews with experts at the company that fog could occur locally and not necessarily on the entire surface, any sensing method that only viewed a local and small section of the glass was somewhat disregarded.

Another problem with the IR sensor was that it was difficult to find what type of sensor that would be suitable for this application. Since it is also used the detect airborne mist in addition to condensation. Since both of these types of sensors are denoted infrared fog sensors, it was difficult to find a befitting sensor that measured fog/condensate since most of the sensors appeared to be used to measure fog/mist.

However, further analysis revealed that an IR sensor could perhaps have been useful. For instance, the company discouraged the placement of sensors on the exterior of the device due to the potential degradation of the water-resistant properties of the product. Therefore, an IR could have been placed inside the DUT and perhaps be capable of detecting frost through the glass. This is especially useful since frost is more commonly found on the outside rather than the inside of the glass according to the quality assurance department at the company.

3.5 Concept selection

During the pilot study, four main methods were found in order to detect fog and frost. The methods were evaluated both by studying relevant literature and by performing simpler validation tests, see section 3. The next step was to choose the most promising method and design a more comprehensive test setup in order to simulate more realistic testing scenarios. The reason why each method

was not tested in a truly realistic scenario was that the time to implement a full test setup with data logging and performing tests in a climate chamber is exceedingly time consuming.

Besides the measurement method, the majority of the test setup was already determined since a lot of equipment was either already chosen by the company or the choice was fully arbitrary, meaning the specific choice would not affect the result with any significance. The already determined equipment was a camera and climate chamber on site that could regulate temperature and humidity. Additionally, it was found suitable to use a microcontroller to interface with the chosen sensors.

When choosing a measurement method the criteria listed below were especially considered. Cost and power consumption are not included since each method can be made at a similar and relatively low cost if implemented in production and the power consumption for all methods are relatively similar and mostly dependent on chosen sample frequency, rather than baseline power consumption. Additionally, the power consumption of the sensor itself is not a main concern, as the primary objective is to minimize net power consumption for the camera. Early detection of fog and frost can significantly reduce the time for which the heater is activated, resulting in substantial power savings compared to the sensor's power consumption. To compare the overall performance of the concepts, the following criteria were set up.

- Measurement area: The size of the area over which the sensor can detect condensation.
- Small size: The physical size of the sensor.
- Reliability: The accuracy and consistency of the sensor's readings over time.
- Sensitivity: The ability of the sensor to detect even small amounts of condensation.
- Early detection: The ability of the sensor to detect condensation as soon as it begins to form or before.
- Resistant to false triggers: The ability of the sensor to avoid false triggers caused by factors other than condensation or frost.

From these criteria, a table was made to visualize the advantages and disadvantages of each method. The determined score for each criterion for every method was chosen mainly from observations made during the testing and validation of sensors. The scoring may also take into account diverse inputs from examining literature and product specifications. This is done to avoid relying solely on anecdotal observations made in this study and instead complement them with more thorough testing from other sources.

- 0 Baseline
- + Relative advantage

- - Relative disadvantage

Table 3.1: Comparison table for the suggested fog and frost detection methods.

	Detect area	Small size	Reliability	Sensitivity	Early detection	Resistant to false triggers
Capacitance	-	+	-	0	-	-
Resistance	-	+	-	-	-	0
Hygrometry	+	0	+	0	+	+
IR	-	-	+	+	0	-

Based on the evaluation criteria and the results obtained from the pilot study, hygrometry was selected as the most promising method for detecting fog and frost. The advantages of hygrometry over the other methods from table 3.1 include:

- **Detection area:** Hygrometry can detect fog on the entire surface, rather than only locally, providing a more comprehensive understanding of the presence of fog compared to localized measurements.
- **Potential for early detection and prevention:** Hygrometry may predict fog and therefore prevent it, lowering the power consumption for the camera's heating element, as removing fog after it has formed requires more energy.
- **Flexible placement:** Hygrometry sensors may not be the smallest solution but can however be placed more liberally, as they do not need to be placed exactly where fog forms. This ensures that the sensor does not obstruct the camera's view.
- **Direct water content measurement:** Hygrometry directly measures water content, providing an accurate assessment of fog without being affected by other contaminants such as dirt.
- **Miscellaneous categories:** Overall, hygrometry performs well or at least not poorly in other aspects, such as power consumption, cost, sensitivity and complexity.

However, one drawback of hygrometry is that it only measures inside the camera, as opposed to infrared and capacitance which can measure through the glass. The outside though, is primarily affected by frost in outdoor camera applications. Despite this limitation, the benefits of hygrometry in terms of comprehensive fog detection, potential prediction of fog, flexible sensor placement, and direct water content measurement make it a valuable solution for maintaining camera performance and visibility under fog and frost conditions.

Finally, the choice of hygrometry as the preferred method for fog detection was deemed to align the most with the goals of this study, see subsection 1.2, providing a predictive measurement in order to lower power consumption, maintaining high reliability, can be incorporated relatively inexpensive and has a relatively small form factor.

Chapter 4

Method

This chapter goes into detail about the performed tests and how they were developed. The outline of the chapter is as follows: A description of the test setup in both hardware and software, insights on why and how the tests were designed and executed, a brief description of the main tests performed and finally the method used to analyze the resulting data.

4.1 Detecting and predicting fog by using hygrometry sensors

From this point the primary focus had shifted away from frost towards a more concentrated study on fog, see section 1.1. The basis of detecting and predicting fog by using combined temperature and hygrometry sensors is to use real time data of the current climate inside the device and compare it to a theoretical psychrometry model. By doing so, it is possible to get an estimate of how close a surface is to becoming foggy. This requires sensors that can measure psychrometric units such as temperature and humidity alongside software that can perform appropriate data handling and calculations.

4.1.1 Test setup

The test setup could be built in many variations which could impact the test results. However, regardless of the exact choices of certain components, the setup will minimally have to consist of a device (an camera) to test, a suitable climate to install the device in, sensors to record measurements and a data processing device such as a computer and microcontroller. Below are specified the components used in this study and therefore the chosen test setup variation.

Hardware

The final choice of required equipment took careful consideration to find. In order to measure the climate inside of the DUT (device under test), the SHT85 temperature and humidity sensor was chosen, seen in figure 4.1a. This was due to several factors but mainly due to the small form factor,

high accuracy and the on-board serial I2C communication. The SHT85 is able to transmit data regarding real time temperature and relative humidity to a microcontroller.

An issue with the SHT85 is that it has a non-changeable default communication address. This makes communicating with multiple SHT85 through the same microcontroller more complicated. If the sensors would have unique identifiers, they can be connected through a shared communication line, known as a bus. Here, the microcontroller unit (MCU) can select the specific sensor it wants to engage with by transmitting that sensor's unique address, thus simplifying the overall communication process. This is not possible if all sensors have the same address. To solve this issue, an I2C multiplexer (MUX) was used in between the sensors and the MCU, seen in figure 4.1b. The MUX acts as a bridging device that switches which sensor is allowed to communicate with the MCU, one at a time.

Together with the SHT85, a pt100 temperature sensor alongside an amplifier with serial communication capability (Adafruit MAX31865) was used to measure the inside glass temperature. The pt100 is a widely used resistance temperature detector and was found suitable due to its high accuracy and reliability. One concern was that the length of wire from the amplifier to the pt100 would interfere with the measurements, mainly because the amplifier measures the resistance of the pt100 and consequently also the connecting wires. This could be solved by using four wires instead of two and therefore measuring and subtracting the wire resistance. Luckily, testing revealed that the wires merely interfered with a practically static offset and could be compensated for in later calculations. This was not a concern with the SHT85 because the serial communication logic was integrated on-board the sensor, thus disregarding wire length as possible interference with the measurements. After early tests, the pt100 along with the amplifier was removed completely and replaced by another SHT85. This was not only done in order to add an additional humidity measurement but also to allow better comparison between glass and climate temperatures by using the same model of sensor.

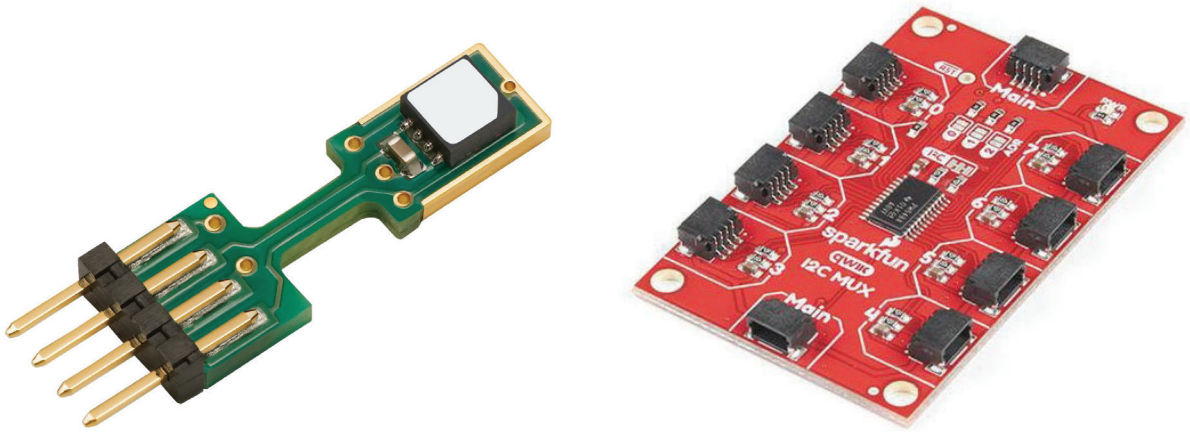

(a) (b)

Figure 4.1: Image of the combined temperature and humidity sensor and the multiplexer used in this study. (a) Sensirion SHT85 temperature and humidity sensor [21].(b) SparkFun I2C Mux (TCA9548A) [10].

The chosen device to test was a camera from an internal department at the company that had specified interest in increased protection against frost and fogging. The camera also had a controllable built in heater and three fans along with plenty of space inside the camera to mount any sensors, making the product nearly ideal for testing fog and frost detection.

Other used equipment includes a microcontroller board such as the Arduino nano 33 IoT to log the sensor data and send it to a computer for analysis, a climate chamber provided by the company, a separate camera as well as other miscellaneous equipment such as power supplies, cable ties, ethernet cables et cetera. The separate camera was used to record the main device from an external perspective and monitor fog build up. This camera was able to do so without experiencing issues with fog since it did not have a dome cover.

Since some equipment is placed in a high humidity environment there is a risk of electrical shortage, such as between the pins on the Arduino, which could damage the equipment. To reduce the risk of having a power shortage between the pins on the Arduino, two extra circuit boards to connect all the sensor probes were constructed and the Arduino and the probe board were connected via an ethernet cable, see figure 4.4.

Hardware Assembly

The hardware setup remained relatively unchanged during the entire study except for a few changes such as removing the pt100 temperature sensor and adding a total of four SHT85 hygrometer sensors. The final setup on the outside of the climate chamber consisted of a personal computer and

a custom made ethernet interface for an Arduino. This was connected via an ethernet cable to the inside of the climate chamber to another custom ethernet interface. The internal interface was, in turn, connected to an I2C multiplexer and four SHT 85 sensors which in total could collect eight values, two values for each sensor, logged every second. Figures 4.2 and 4.3 show the assembled setup, where the first figure is assembled outside of the climate chamber and the latter of an early test inside the chamber.

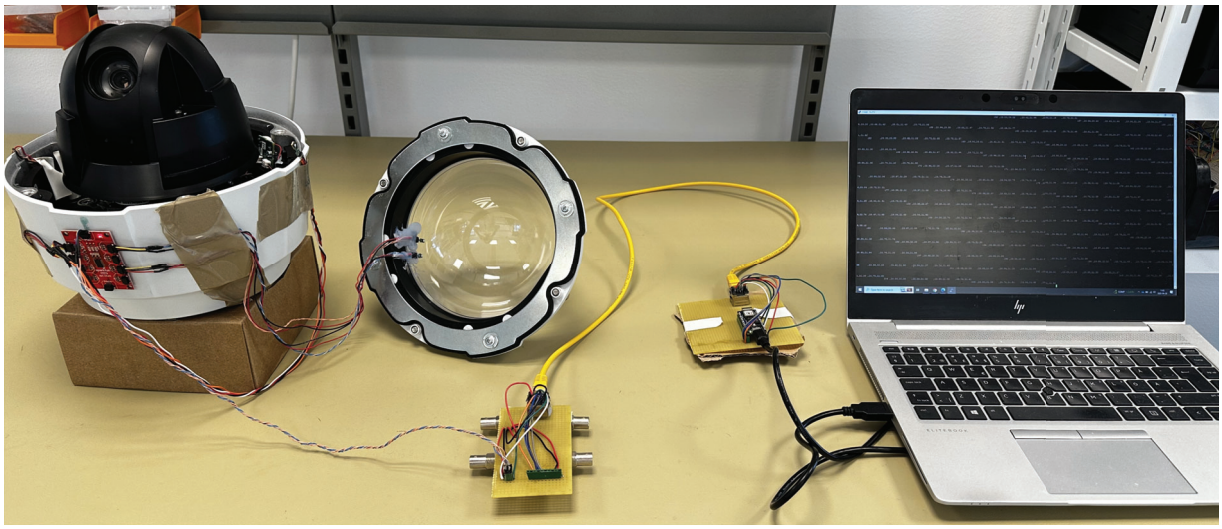

Figure 4.2: Picture of the setup made to log data from four SHT85 sensors. Note, the picture is taken outside a climate chamber and the dome cover open for demonstrative purposes.

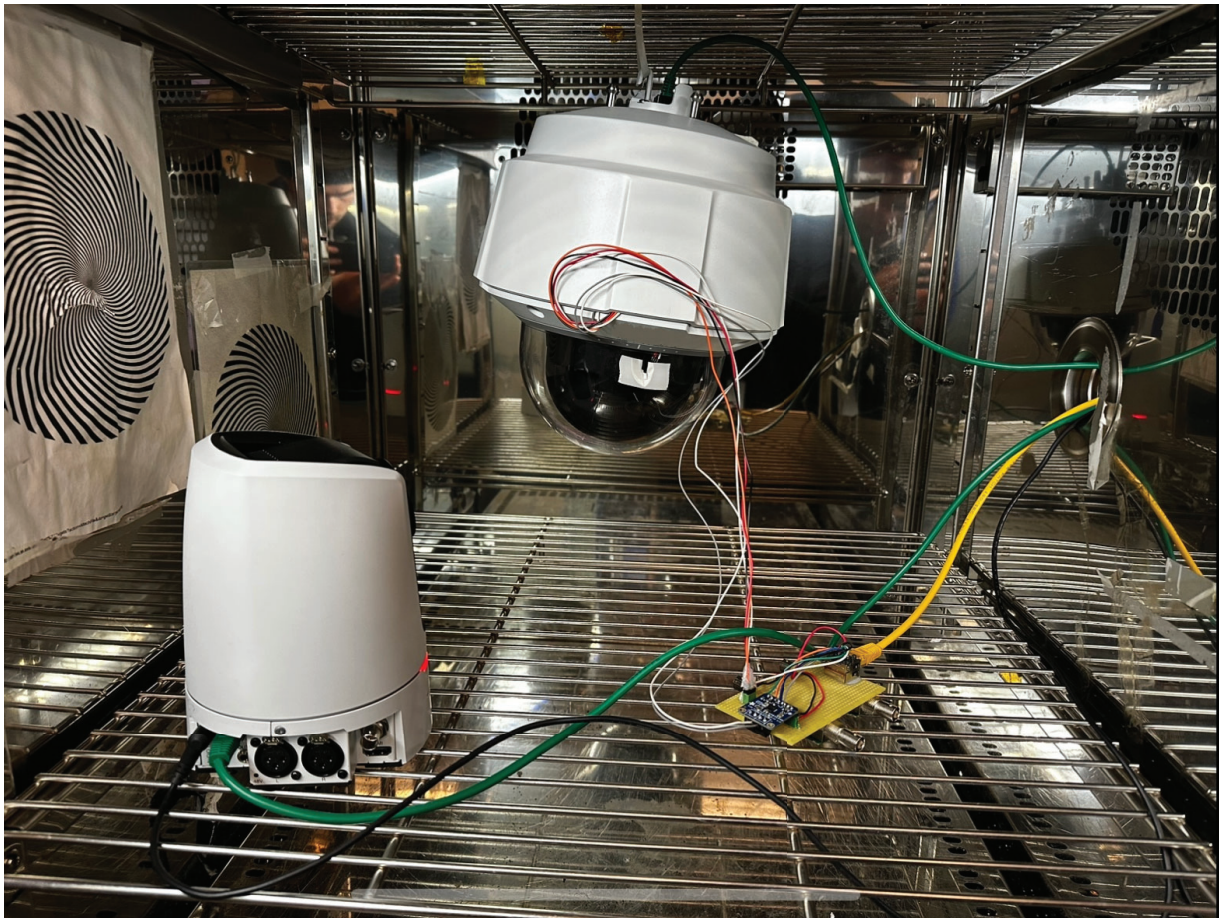

Figure 4.3: Picture of the test setup during an early test.

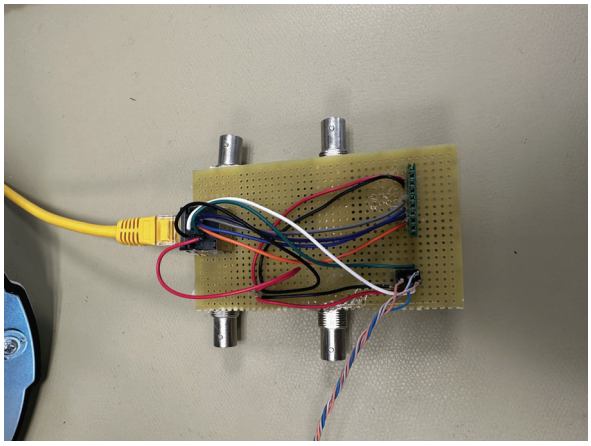

(a) Ethernet to Multiplexer interface

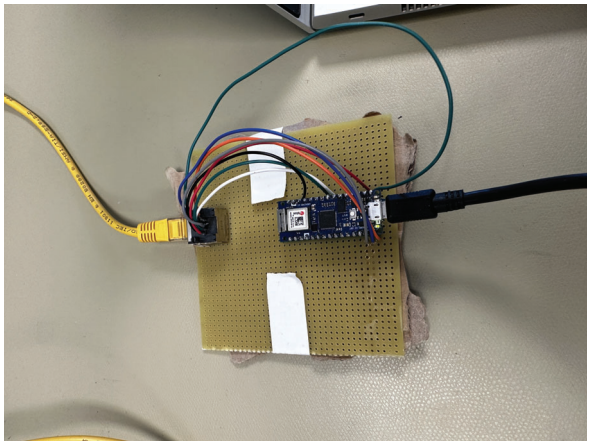

(b) Arduino to Ethernet interface.

Figure 4.4: Custom made ethernet interfaces made on perfboard. The interfaces makes it possible to use commercial ethernet cables at various lengths depending on use case.

The arrangement of the four SHT85 temperature and hygrometry sensors is illustrated in figure

4.5, with each sensor strategically placed to capture comprehensive data from different points of interest. The first sensor, positioned at the center of the device, monitors the average internal climate conditions of the DUT, balancing proximity to heat generating components and the device's colder regions. The second sensor is situated externally and records the ambient environmental conditions surrounding the device. The third sensor is affixed directly to the inside glass surface, while the fourth sensor is placed approximately 2mm away from the glass, to measure climatic conditions adjacent to the glass.

Figure 4.5: Image of the device under test with four SHT85 sensors. To make the sensor locations easier to identify, green circle markers have been added to the image.

Software

Due to the use of multiple types of hardware on multiple platforms, it was necessary to format and gather all data onto a single platform for comparison and analysis proposes. This had to be done in an automated fashion due to the millions of data points from each test. This was done by separating the logic into three fields: External sensors, device system logs and external video recording camera.

The external sensors, which measure internal DUT temperatures and humidity, communicate with an Arduino microcontroller (MCU) via a multiplexer (MUX) through the I2C serial communication protocol. The MCU communicates to the MUX regarding which sensor to read from, formats and prints the data to the serial output. Source code for the Arduino can be seen in appendix A. The serial output is then logged by a desktop computer and stored in a text file as raw data. Once the test is complete, a Python script converts the data from the text file neatly into a CSV file format which is readable by most commercially available spread cheat software such as Microsoft Excel. Source code for the Python script can be seen in appendix B.

The device under test has internal system reports with time stamps of key events. These reports were meant to be logged automatically by software provided by the company but unfortunately malfunctioned during the time of this thesis. The solution was to manually enable and record system logs of key events such as enabling the heater and fans.

Finally, during the tests, an additional camera was used to record videos of the DUT. These recordings were manually analyzed in order to note times when the fog was present and to which extent. A visualization of the data flow can be seen as a flowchart, depicted in figure 4.6.

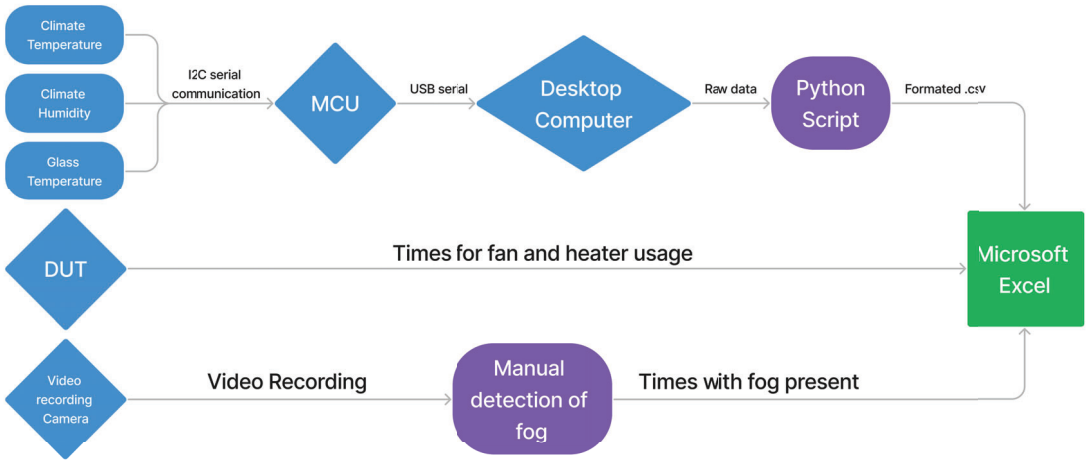

Figure 4.6: Simplified flow chart of test setup data flow.

4.2 Test procedures and insights

This section presents the conducted tests to predict and detect fog occurrence inside the device under test (DUT). The focus lies on both outlining the early test methodology and design as well

as performing final testing. The early findings proved to be crucial in refining the testing process. Challenges faced during the testing phase, along with the steps taken to improve data analysis, will be discussed in detail. By comprehending the limitations and possibilities of psychrometry in real world scenarios, the ultimate goal is to develop an optimized approach for fog detection in the device. The section provides a comprehensive overview of the challenges and findings with the experimental setup, data collection, analysis techniques, and key decisions made during the testing phase.

4.2.1 Test methodology and design of early tests

The goal of these tests was to predict and detect when fog may occur inside the DUT. This involved taking three measurements: temperature and humidity inside the DUT along with the glass temperature. The temperature and humidity inside the DUT can be used to calculate the current dew point temperature. If the glass temperature falls close to or below the dew point temperature, the risk of condensation is increased. Hence, the glass temperature serves as a measurement to identify scenarios of high risk for condensation.

However, prior to data gathering and analysis, a testing methodology and design outline had to be established. This involved tasks such as becoming familiar with the equipment, ensuring that data logging was working properly, and testing various timings, temperatures, and other parameters. These tasks were necessary to ensure that the tests were conducted properly and to minimize the potential for errors in the data.

4.2.2 Testing process

In order to validate the strategy of predicting fog using psychrometry, multiple tests were performed over a number of weeks, each test taking between 8-40 hours. The reason for these tests was to get a practical understanding of the test setup as well as to prepare for and design future tests. For instance, without any prior knowledge, it can be difficult to even create a scenario where fog is produced. Initial attempts were done by acclimatizing the DUT in a high temperature and humidity environment followed by suddenly reducing the outside temperature to generate fog. However, multiple parameters still need to be considered since they will influence the outcome, such as:

- Time to acclimatize.
- Start and end temperature and humidity.
- Having the DUT powered on or off (producing ca 15°C higher DUT temperature).
- Whether to enable heaters and fans or not.

- Timings for all test events.

The time to acclimatize the DUT was time consuming, especially so regarding humidity. For instance, going from a general indoor climate to placing the DUT in a chamber at 50°C 90% RH repeatedly resulted in the DUT temperature equalizing under two hours. However, the humidity came close to steady state minimally after approximately 20 hours. Consulting with an expert from hardware quality assurance revealed that a recommended practice at the company was to leave the DUT in the climate chamber for 24h. This became an obstacle due to the large number of tests that needed to be performed. To combat the long acclimatization times regarding humidity, the DUT was purposefully left slightly open until the humidity inside the DUT was equal to the surroundings. At this point, the DUT was sealed and left to acclimatize further. This altered the preparation times to around 3h opened and 2h sealed, resulting in a circa 5 times faster acclimatization.

In order to maximize the probability of fog to occur, the climate was set to 50°C 90% RH and after acclimatization reduced rapidly to 3°C with humidity controlled disabled. Controlling humidity during the temperature drop was regarded as counterproductive since it would inhibit the temperature control to provide maximum cooling when also controlling humidity. To maintain consistency in the testing process, the same start and end conditions, along with timings, were applied throughout the initial tests. This strategy reliably produced fog and ensured that only one parameter varied between each test, enhancing the clarity of the results.

After only a few preliminary tests it was found that additional data could prove useful to get a better idea of what was happening at different time periods. Initially, only the values from the temperature and humidity sensors were recorded which were difficult to analyze on their own. The additional data that could be collected and compared to the sensor values were camera recordings to manually detect when fog occurred, real time values for temperature and humidity inside the climate chamber and logs of time stamps for fan and heater usage. Therefore, this additional data was also collected to further the analytic capabilities.

Calculating the dew point and comparing it to the glass temperature tended towards a lower difference during fogging, which was a result of potential. However, at least during early tests, before the analytic model was refined, the difference was not large enough to simply set a threshold in order to detect fog. Perhaps a more advanced data analysis model with regard to hysteresis could accurately predict when condensation occurred, but more likely the test setup could be improved first. Therefore, testing continued with the purpose of understanding the system better in order to optimize the data output. Some key areas to investigate were:

- Placement of sensors.
- Climate fluctuations inside DUT.

- Which local temperature to use when calculating the dew point.
- Temporary relative humidity drop instead of rise when the outside temperature dropped.
- Removing trapped moisture between tests.
- Importance of humidity level.
- Accuracy and precision of temperature and humidity sensors.
- How ambient temperature and humidity affect the severity of fogging inside the DUT.

The initial plan was to conduct early tests followed by definitive final tests. However, due to the complexity and unpredictability associated with a multitude of factors, the transition between the initial and final stages was not distinct. The approach was thus to continuously test with each test bringing improved clarity and insights. As the process evolved, the testing methods became more sophisticated and standardized. The test objectives were refined, aligning more closely with the goals of the study, to detect fog in simulations of real world scenarios.

Throughout the testing phase, a range of challenges were faced which invalidated certain tests, such as hardware malfunctions, unforeseen system reboots, forgetting to record data et cetera. However, the majority of tests were somewhat to fully successful in regards to recording useful data and progressing the general knowledge. These tests are described, motivated and commented on in Table 4.1.

Table 4.1: Summary of tests

I	Elapsed time	26h:54m
	Conditions	The camera was preconditioned with the camera lid closed. During the test the camera was turned off, T50°C RH90% $\rightarrow$ T3°C RH:OFF
	Specific Goals of test	* Is this temperature and humidity difference sufficient to generate fog. * How long does it takes for the temperature and humidity to reach steady state.
	Comments	Without remark

II	Elapsed time	24h:24m
	Conditions	The camera was preconditioned with a closed lid. The Camera was turned on during the test and the heater and fans were turned on in the GUI manually every hour. T50°C RH90% $\rightarrow$ T3°C RH:Off
	Goals of test	* Is there a big difference between when the camera is off compared to when the heater and fan are turned on in the GUI. * Does fog form when the heater is on in the GUI
	Comments	Manual test, assumably badly performed by the operator
III	Elapsed time	26h:54m
	Conditions	The camera was pre conditioned with the lid opened, the camera was turned off during the test, T50°C RH90% $\rightarrow$ T3°C RH:Off
	Goals of test	* can the preconditioning process of the camera be done faster by having the lid open *How long does it takes to reach steady state when the lid is pre-conditioned with the lid open
	Comments	Without remark
IV	Elapsed time	22h:52m
	Conditions	The camera was pre conditioned with the lid opened, the camera was turned off during the test, T50°C RH90% $\rightarrow$ T3°C RH:Off
	Goals of test	* Check the repeatability of the test. In other words, are the same result achieved if the test is repeated.
	Comments	Wrong test performed due to disconnected power supply, the power was suppost to be on. However, gave valuable information regarding the repeatability of the test.
V	Elapsed time	24h:00m
	Conditions	The Camera was pre conditioned with the lid opened. It was then closed and kept for about an hour before the cooling process was initialized. When the cooling process was initialized the reference value for the temperature was set to the lower temperature and the humidity control of the climate chamber was turned off. The camera was on during the whole operation. T50°C RH90% $\rightarrow$ T3°C RH:Off
	Goals of test	* Check how the parameters, humidity and temperature are affected by that the camera is turned on during the operation and whether or not condense will form while the camera is on
	Comments	Without remark

VI	Elapsed time	18h:11m
	Conditions	The Camera was pre conditioned with the lid opened. It was then closed and kept for about an hour before the cooling process was initialized. When the cooling process was initialized the reference value for the temperature was set to the lower temperature and the humidity control of the climate chamber was turned off. The camera was turned off during the whole operation. T50°C RH30% $\rightarrow$ T3°C RH:Off
	Goals of test	* Check how the parameters, humidity and temperature is affected by having a lower humidity in the chamber and to see whether condense will form in this scenario
	Comments	The origional intention for this test was to see how the parameter inside the camera would react if the ambient humidity was lower than 45 % compared with the usual 90%. However, when the lid was shut after the pre conditioning the Arduino shut down, from a potential overcurrent protection. The camera had to be taken out of the climate chamber in order to fix the problem. Furthermore, that resulted in that there was not enough time to precondition to the original 45% instead the humidity was lowered to 30%. However, it was deemed better to perform the test anyways to get some data instead of having to Waste a full day of testing, even though the test result might not be as reliable.
VII	Elapsed time	20h:01m
	Conditions	Camera was pre conditioned with the lid opened. It was then closed an kept for about an hour before the cooling the temperature was dropped and the humidity control of the climate chamber was turned off. The camera was turned off during the whole operation. T50°C RH45% $\rightarrow$ T3°C RH:Off
	Goals of test	* Check how the parameters, humidity and temperature are effected by having a lower humidity, 45%, in the chamber and to see whether condense will form in this scenario
	Comments	Without remark

VIII	Elapsed time	24h:10m
	Conditions	Camera was preconditioned with the lid opened. It was then closed and kept for about an hour before the cooling process was initialized. When the cooling process was initialized the reference value for the temperature was set to the lower temperature and the humidity control of the climate chamber was turned off. The camera was turned off during the whole operation. T50°C RH90% $\rightarrow$ T3°C RH:90%
	Goals of test	* See if the humidity near the glass would decrease as much when then ambient humidity was kept at 90% during the cooling * Will this have an effect on the amount of fog that is formed.
	Comments	The climate control could not keep the humidity high during the cooling process. Resulting in that at the end of the test, the humidity was $\tilde{3}$0% in the climate chamber
IX	Elapsed time	20h:42m
	Conditions	The Camera was keep open and on overnight T50°C RH90%
	Goals of test	* Evaluate how long it takes to reach steady state while the lid is opened. * Check if calculated absolute humidity is the same for all sensors inside the camera.
	Comments	Without remark
X	Elapsed time	3h:16m
	Conditions	Camera was pre-conditioned with the lid open and the camera on during the night. The camera was then closed and kept for about an hour before the cooling process began. During this hour the fan and heater were turned on in the GUI and it was kept on during the cooling process. T50°^{C} RH90% $\rightarrow$ T3°^{C} RH:Off
	Goals of test	* Repeat test when the heater and fan were turned on in the GUI during the cooling (Since the last test was not carried out properly). * Will this have an effect on the amount of fog that is formed.
	Comments	Without remark
XI	Elapsed time	22h:59m
	Conditions	The camera was pre conditioned with the lid opened. The lid was then kept open during the cooling process: T50°C RH90% $\rightarrow$ T3°C RH:Off
	Goals of test	* Evaluate how the parameters would be affected if the lid was opened during the entire test, not only during acclimatization. * See if this has an effect on the amount of fog that is formed.
	Comments	Without remark

XII	Elapsed time	21h:40m
	Conditions	The camera was pre conditioned with the lid opened. It was then closed and kept for about an hour before the cooling process was initialized. When the cooling process was initialized the reference value for the temperature was set to the lower temperature and the humidity control of the climate chamber was turned off. The camera was off during the operation: T50°C RH90% $\rightarrow$ T3°C RH:Off
	Goals of test	* Get all four sensor data for the "base case".
	Comments	Without remark

4.2.3 Data analysis

To analyze the data from the experiments, the data was transferred into Excel via a Python script. The collected data from the sensors and Arduino microcontroller was elapsed time in seconds and humidity and temperature from four different sensor probes making it a total of 9 values per measurement. To simplify and streamline the analysis of the data, the following steps were implemented:

- Firstly, to make the handling of the data easier, time logs were converted to display in hours, minutes, and seconds, both in the formats of time elapsed from the start of the test, and real time of day.
- Secondly, from the collected sensor data several key values were calculated such as the dew point temperature, absolute humidity and dew point minus the glass temperature which may also denoted as "fog value". The final version of the Excel sheets can be seen in 4.7. The columns E-M are measured input values and the rest are calculated based on the input.
- Thirdly, several different approximations of the dew point were tested to see whether it made a notable difference in the results.
- Since the collected data consisted of a major set of data points, they were mostly analyzed graphically to visualize trends and simplify analysis.
- A Python program was utilized to illustrate data points within a psychrometric chart, See appendix C. However, it is important to note that psychrometric charts do not inherently convey information regarding time, thus it can be difficult to understand where the beginning and end of the test are. The data was therefore cut to only display the information during and after the cooling process, hence ignoring the heating process of the system.

C	D	E	F	G	H	I	J	K	L	M	N	O	P	Q	R	S	T
Elapsed Time [hh:mm:ss]	Real Time [hh:mm:ss]	Arduino Time [s]	T_out [C]	RH_out [C]	T_glass [C]	RH_glass [%]	T_nearGlass [C]	RH_nearGlass [C]	T_inside [C]	RH_inside [%]	Calculated dew point near glass [C]	Calculated dew point inside camera [C]	Dew point near glas vs Glass temp [C]	Dew point inside the camera vs glas temp [C]	AH Near glass [g_water/kg_air]	AH outside [g_water/kg_air]	AH inside [g_water/kg_air]
00:00:00	00:00:00	2	23.85	37.9	20.54	40.88	20.52	40.76	20.13	41.38	6.689777641	6.558609121	13.85022236	13.98139088	7.253695747	8.194266358	7.195689291
00:00:01	00:00:01	3	23.9	37.92	20.59	40.9	20.51	40.76	20.12	41.4	6.68084747	6.556618697	13.90915253	14.0333813	7.249401677	8.222258269	7.194893588
00:00:02	00:00:02	4	23.96	37.89	20.59	40.88	20.51	40.81	20.19	41.46	6.698510327	6.640086602	13.89148967	13.9499134	7.258294466	8.244208655	7.235326391
00:00:03	00:00:03	5	24.1	37.9	20.62	40.93	20.5	40.85	20.15	41.53	6.703694271	6.62858981	13.91630573	13.99141019	7.261107385	8.313123233	7.230353934
00:00:04	00:00:04	6	24.16	37.83	20.63	40.93	20.41	40.84	20.15	41.58	6.619778196	6.645915698	14.0102218	13.9840843	7.220728162	8.32645826	7.239058911
00:00:05	00:00:05	7	24.23	37.88	20.66	40.94	20.47	40.86	20.19	41.6	6.68042379	6.688637875	13.97957621	13.97136212	7.249991225	8.371084473	7.25975827
00:00:06	00:00:06	8	24.36	37.66	20.69	40.89	20.4	40.99	20.2	41.68	6.663645074	6.725265808	14.02635493	13.96473419	7.24295533	8.384846044	7.27803761
00:00:07	00:00:07	9	24.43	37.76	20.6	41.02	20.44	40.85	20.09	41.67	6.650100795	6.623349229	13.9498992	13.97665077	7.235346493	8.440952537	7.228926028
00:00:08	00:00:08	10	24.46	37.74	20.67	40.93	20.45	40.9	20.19	41.76	6.676653936	6.743943563	13.99334606	13.92605644	7.248495627	8.451012861	7.287680417
00:00:09	00:00:09	11	24.43	37.71	20.69	40.95	20.5	40.89	20.17	41.83	6.717796959	6.750170759	13.97220304	13.93982924	7.268217405	8.429775429	7.291235543
00:00:10	00:00:10	12	24.54	37.7	20.62	40.89	20.5	41.07	20.19	41.91	6.7811043	6.795618024	13.8388957	13.82438198	7.300212492	8.480867745	7.31385743
00:00:11	00:00:11	13	24.6	37.53	20.73	40.89	20.5	40.89	20.17	42.14	6.717796959	6.85660477	14.01220304	13.87339523	7.268217405	8.471701118	7.345270519
00:00:12	00:00:12	14	24.77	37.69	20.7	40.73	20.5	40.97	20.12	42.21	6.74596476	6.835727203	13.95403524	13.8642728	7.282437444	8.591012316	7.335663245
00:00:13	00:00:13	15	24.81	37.69	20.73	40.69	20.52	40.92	20.15	42.26	6.746233213	6.879686967	13.98376679	13.85031303	7.282169529	8.610686701	7.357446599
00:00:14	00:00:14	16	24.94	37.5	20.72	40.68	20.52	40.88	20.12	42.4	6.732138153	6.900491824	13.98786185	13.81950818	7.275051083	8.631159348	7.368683288
00:00:15	00:00:15	17	24.87	37.56	20.8	40.47	20.5	40.99	20.13	42.42	6.7529989	6.916260833	14.0470011	13.88373917	7.285992453	8.610467451	7.376537934
00:00:16	00:00:16	18	24.87	37.58	20.72	40.53	20.52	40.91	20.24	42.61	6.742710623	7.079419095	13.97728938	13.6405809	7.280389917	8.615052364	7.458113041
00:00:18	00:00:18	20	25.01	37.58	20.77	40.47	20.57	41.02	20.24	42.64	6.826095591	7.089582891	13.94390441	13.68041711	7.321606703	8.684208845	7.463364001
00:00:19	00:00:19	21	25.04	37.61	20.75	40.48	20.55	40.84	20.17	42.79	6.744826303	7.077481525	14.0051737	13.67251847	7.280853572	8.706033096	7.458569661
00:00:20	00:00:20	22	25.2	37.65	20.79	40.44	20.58	41.02	20.15	43	6.83503143	7.130231502	13.95496857	13.6597685	7.325941672	8.795161865	7.486280259
00:00:21	00:00:21	23	25.31	37.45	20.83	40.3	20.47	40.85	20.19	43.07	6.676897608	7.189650966	14.15310239	13.64034903	7.248216876	8.803413382	7.516292997
00:00:22	00:00:22	24	25.32	37.42	20.87	40.41	20.55	40.78	20.19	43.17	6.72363734	7.22316598	14.14636266	13.64683402	7.270156922	8.801369028	7.533744339
00:00:23	00:00:23	25	25.38	37.43	20.86	40.48	20.64	40.91	20.21	43.28	6.849911392	7.277921039	14.01008861	13.58207896	7.332283588	8.833825987	7.561911233
00:00:24	00:00:24	26	25.49	37.47	20.96	40.9	20.59	41	20.19	43.29	6.836933812	7.263290925	14.12306619	13.69670908	7.326704893	8.898741813	7.554685949

Figure 4.7: The final version of the excel document where the data is processed.

Chapter 5

Results

In this chapter, results from twelve tests are presented. The results are presented in graphs and figures, supplemented by explanatory text that conveys information beyond the visual representation. The chapter is structured as follows: A summarizing overview of all test results from tests where two sensors were used followed by when four sensors were used.

5.1 Overview of results

This section provides an overview of the results and explains key concepts. In the following sections, the test results are presented in four reoccurring types of graphs.

The first type shows all raw sensor data plotted over time. This shows how all values of temperature and humidity change over time and provides an overview of the test. An example of this type of graph can be seen in figure 5.8.

The second type shows two graphs of fog value, or glass temperature subtracted by calculated dew point temperature, over time. The difference between the two graphs is that one of the fog values is calculated from the SHT85 sensor in the middle of the camera and the other is from the sensor near, but not on, the glass. This enables comparison between sensor placements. The fog value graphs can be compared to the raw sensor data to spot trends and provide a better understanding of the test. An example of this type of graph can be seen in figure 5.9

The third type shows the temperature difference between the glass and near the glass. This is of secondary significance but provides an understanding of how cold, or hot, the glass surface is compared to the nearby air. This can be used to see how the temperature difference relates to fogging when compared with the other types of graphs. An example of this type of graph can be seen in figure 5.10

The fourth type shows psychrometric movements during the test for the two different sensor placements. This type of graph offers a psychrometric perspective, allowing for interpretations such as a

close horizontal distance from the graph to the saturation line, which can be interpreted as a high potential for fog occurrence. An example of this type of graph can be seen in figure 5.17

During the various tests performed, a varying amount of fog was produced. To streamline the quantification of fog formed, the terms none, small, medium and large were introduced. The terms describe the relative amount of fog produced at the point of maximum condensation during the test. Examples of the fog quantities in relation to the terms can be seen in figure 5.1.

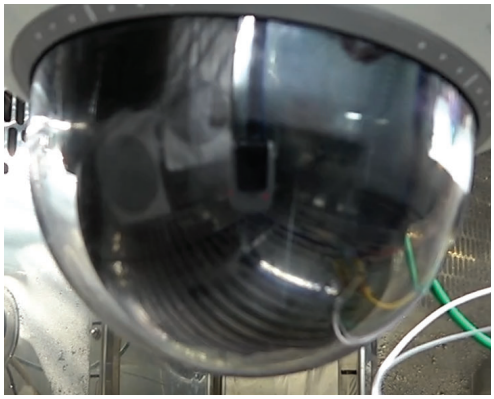

(a) None

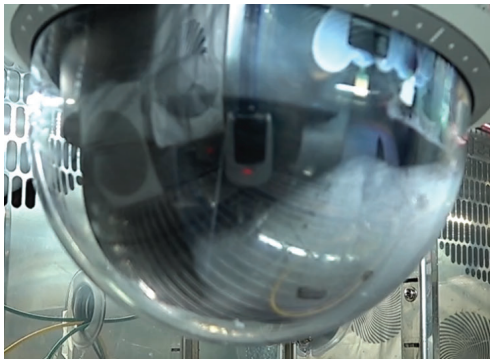

(b) Small

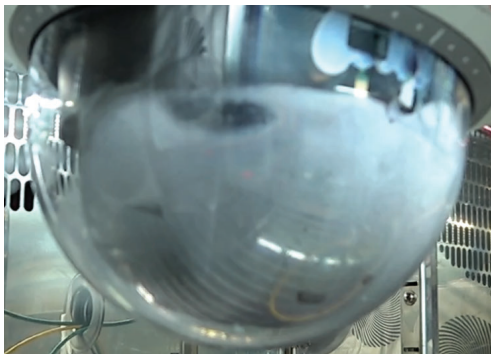

(c) Medium

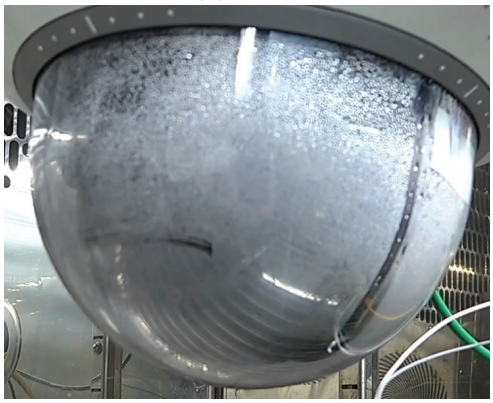

(d) Large

Figure 5.1: Examples of the four fog levels used to quantify fog production during testing.

Table 5.1 presents the results from the twelve key tests I - XII. Presented for each test is the amount of fog formed, whether fog was detected, the amount of fog left once the test was terminated and the findings based on the predetermined goals of the test.

Table 5.1: Result of tests

I	Fog formation	Large
	Fog detected	No
	Amount of fog remaining	Large excess of fog left. A majority of the glass was covered in fog at test completion.
	Findings from goal of test	* The temperature and humidity used in the test, $50°C$ & 90% $\rightarrow$ $3°C$ & Humidity control off, was sufficient to generate fog within the camera. * Temperature steady state was reached within four hours. Humidity steady state was not reached even at test completion; after 21 hours.
II	Fog formation	Medium
	Fog detected	No
	Amount of fog remaining	Medium excess of fog left. A portion of the glass was covered in fog at test completion.
	Findings from goal of test	* After the cooling process, the temperature on and close to the glass was much higher when the camera was powered on (15-20) $°C$ * Fog formed even when the heater was turned on during the cooling process.
III	Fog formation	Large
	Fog detected	No
	Amount of fog remaining	Large excess of fog left. A majority of the glass was covered in fog at test completion.
	Findings from goal of test	* The acclimatization process was much faster when the camera lid was slightly open compared to when it was closed. Approximately 2.5 hours was needed to reach a steady state when the camera was opened. The camera then needed another 1-2 hours to acclimatize after the lid was shut.
IV	Fog formation	Large
	Fog detected	No
	Amount of fog remaining	Large excess of fog left. A majority of the glass was covered in fog at test completion.
	Findings from goal of test	* The test was repeatable. The temperature and humidity curves appeared similar when comparing the two tests

V	Fog formation	Small
	Fog detected	No
	Amount of fog remaining	Slight excess of fog left. A small portion of the glass was covered in fog at test completion.
	Findings from goal of test	* After the cooling process, the temperature on and close to the glass was much higher when the camera was powered on (12-17) $°C$. Meaning, the temperature does not drop as low due to the internal temperature regulation.
VI	Fog formation	None
	Fog detected	No
	Amount of fog remaining	-
	Findings from goal of test	* No fog was formed on the glass cover. The maximum relative humidity was 54.2 $°C$
VII	Fog formation	Medium
	Fog detected	No
	Amount of fog remaining	No fog was visible at the end of the test within the field of view.
	Findings from goal of test	* Fog was formed on the glass cover even at lower relative humidity. The lower amount of produced fog meant that the fog was able to evaporate even during the cooling process.
VIII	Fog formation	Large
	Fog detected	Yes
	Amount of fog remaining	Large excess of fog left. A majority of the glass was covered in fog at test completion.
	Findings from goal of test	* The climate chamber failed to maintain the humidity at 90% thus invalidating the original intention of the test.
IX	Fog formation	-
	Fog detected	-
	Amount of fog remaining	-
	Findings from goal of test	* Steady state was reached after approximately four hours. * As expected, the calculated absolute humidity was nearly identical for all sensors even though the sensors compared to each other displayed very different relative humidity and temperature.

X	Fog formation	Small
	Fog detected	Yes
	Amount of fog remaining	Slight excess of fog left. A small portion of the glass was covered in fog at test completion.
	Findings from goal of test	* No notable difference was observed when the heater was regulated manually compared to when it was regulated automatically.
XI	Fog formation	None
	Fog detected	No
	Amount of fog remaining	-
	Findings from goal of test	* No fog was formed when the camera was opened during the test. * The humidity drop was much higher and occur much earlier in relation to the temperature drop (the humidity drop is less delayed) compared to when the camera is closed. * No fog was observed during the test.
XII	Fog formation	Large
	Fog detected	Yes
	Amount of fog remaining	Large excess of fog left. A majority of the glass was covered in fog at test completion.
	Findings from goal of test	Data from all four sensors were successfully collected for the "base case".

5.2 Tests with two sensors

The tests with two sensors were performed with the pt100 temperature sensor as the T_glass measurement and the SHT85 as the T_nearGlass measurement. The pt100 had a static error of circa $+0.5°C$ due to improper calibration. The error is not taken into account in these graphs since they are meant to display raw data.

Figure 5.2 and 5.5 shows the three sensor values for tests III, and V. For a more detailed description of the tests see table 4.1. The temperatures are plotted in three variants of blue and grey while the humidity is plotted in green

The figures 5.3 and 5.6 shows glass temperature minus the DPT of the sensors called *fog value* for tests III and V. These graphs show the fog values for the sensors placed closed to the glass. The blue curve illustrates the fog value of the sensor near the glass. Note that in these graphs a fog

value below zero in the graphs indicates that fog has been formed.

Figure 5.4 shows the temperature difference between the glass and close to the glass.
Figure 5.7 shows a psychrometric chart of the psychrometric movement of the air, close to the glass cover for tests III and V, during a cooling process.

5.2.1 Tests where the camera is powered off

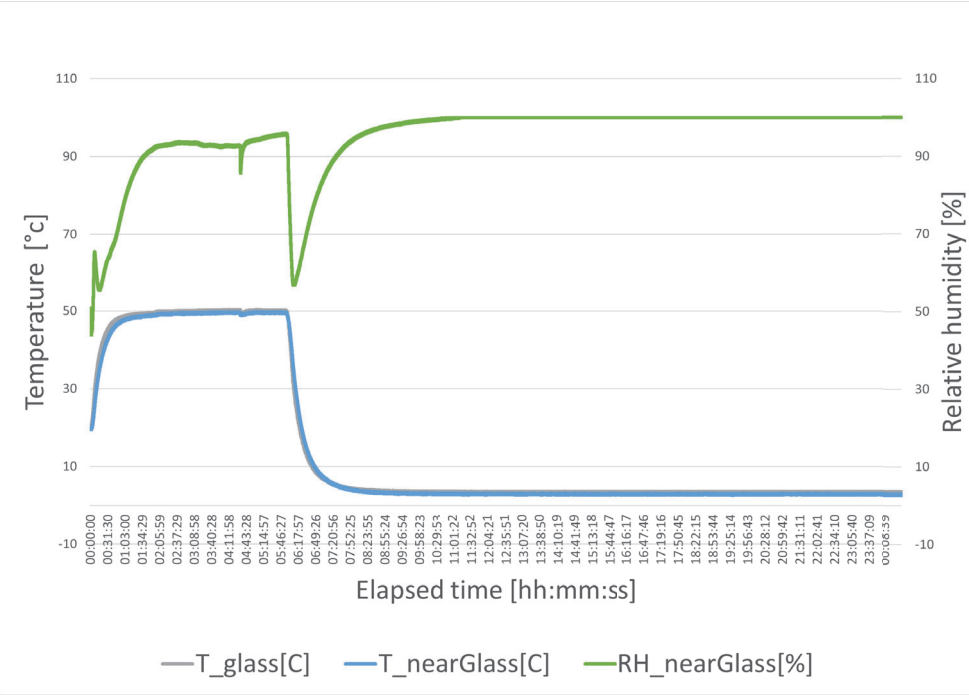

Figure 5.2: All the sensor inputs from test III, the relative humidity and temperature from the two sensors.

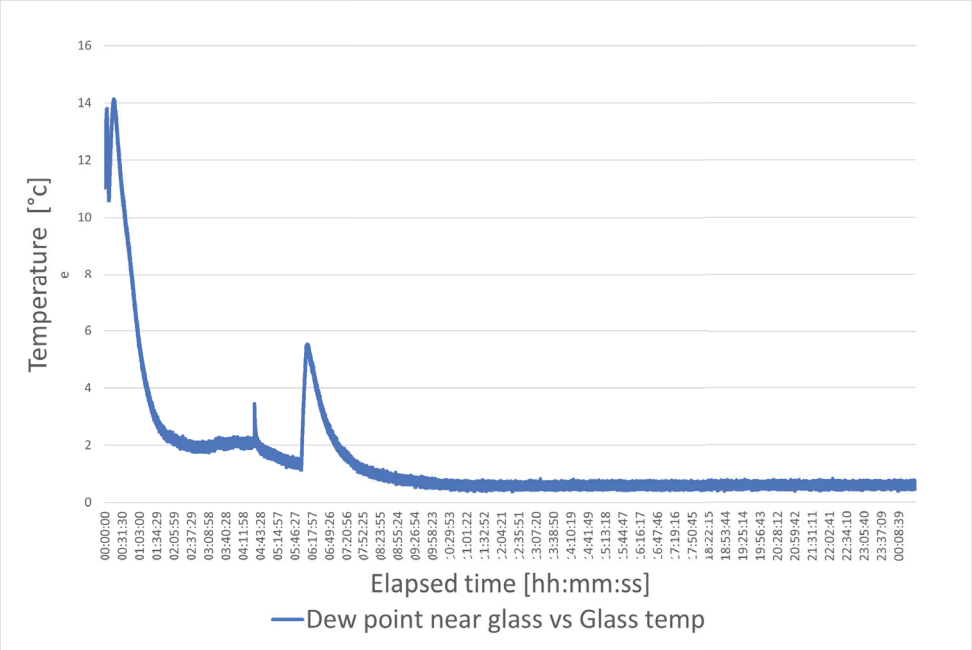

Figure 5.3: The difference between the glass temperature and the dew point temperature for the sensor near the glass and the sensor in test case III.

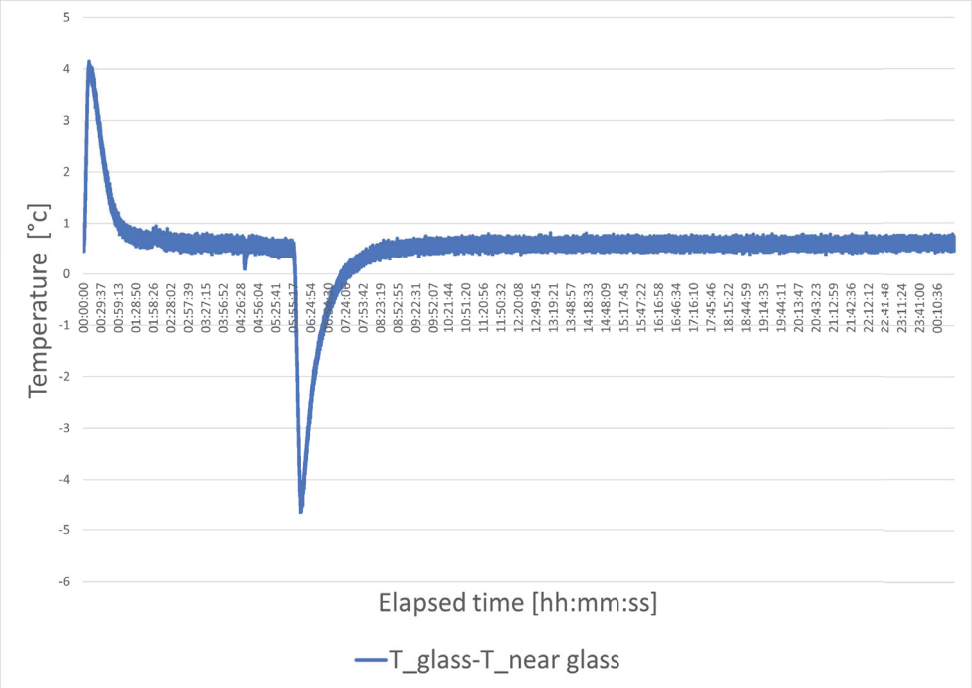

Figure 5.4: Shows the temperature difference between the glass and the near glass for test III.

5.2.2 Tests where the camera is powered on

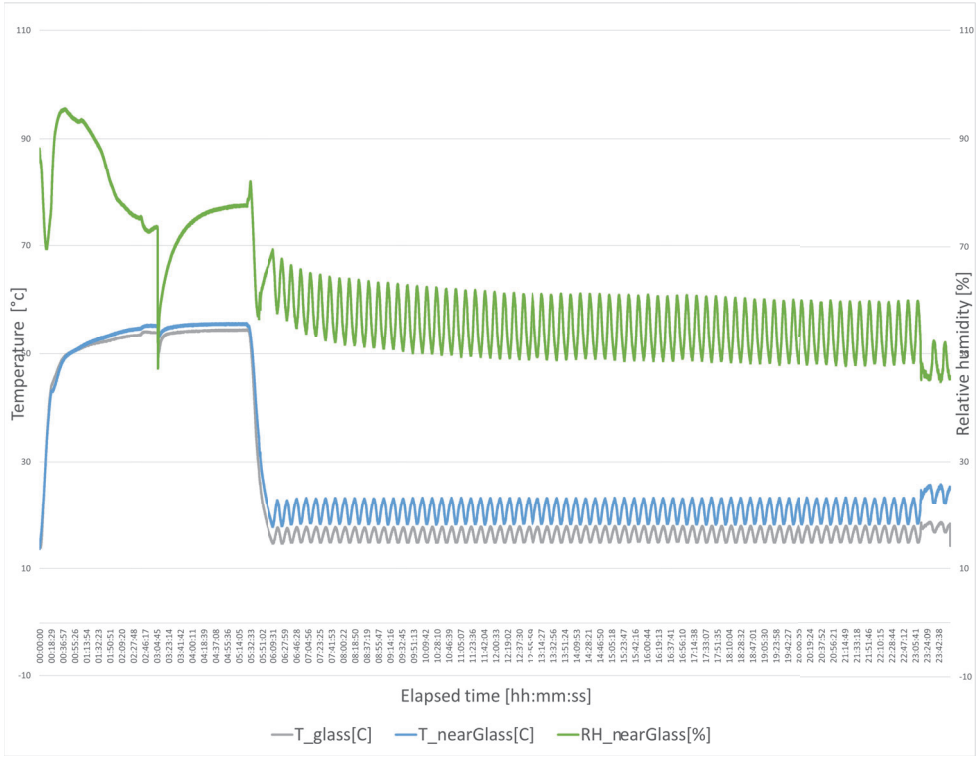

Figure 5.5: All the sensor inputs from test V, the relative humidity and temperature from the two sensors.

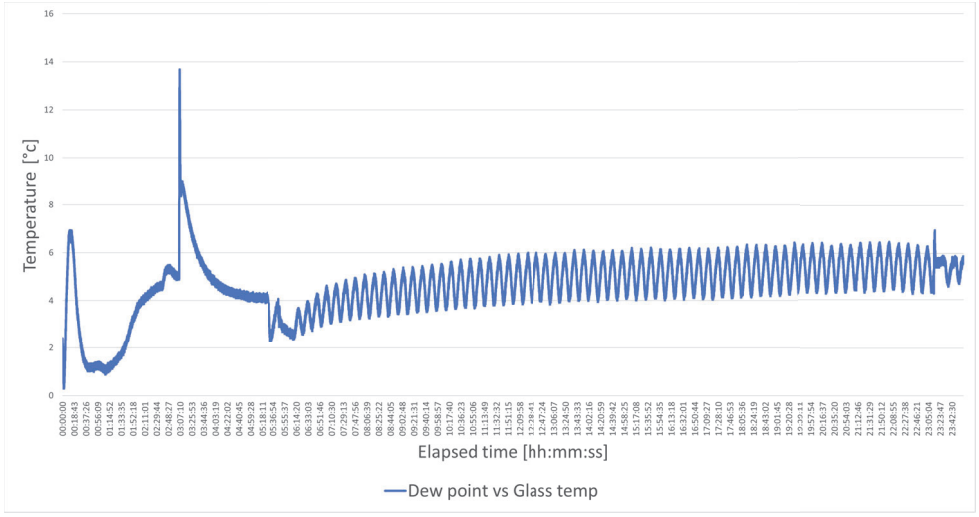

Figure 5.6: The difference between the glass temperature dew point temperature for the sensor near the glass in test case V.

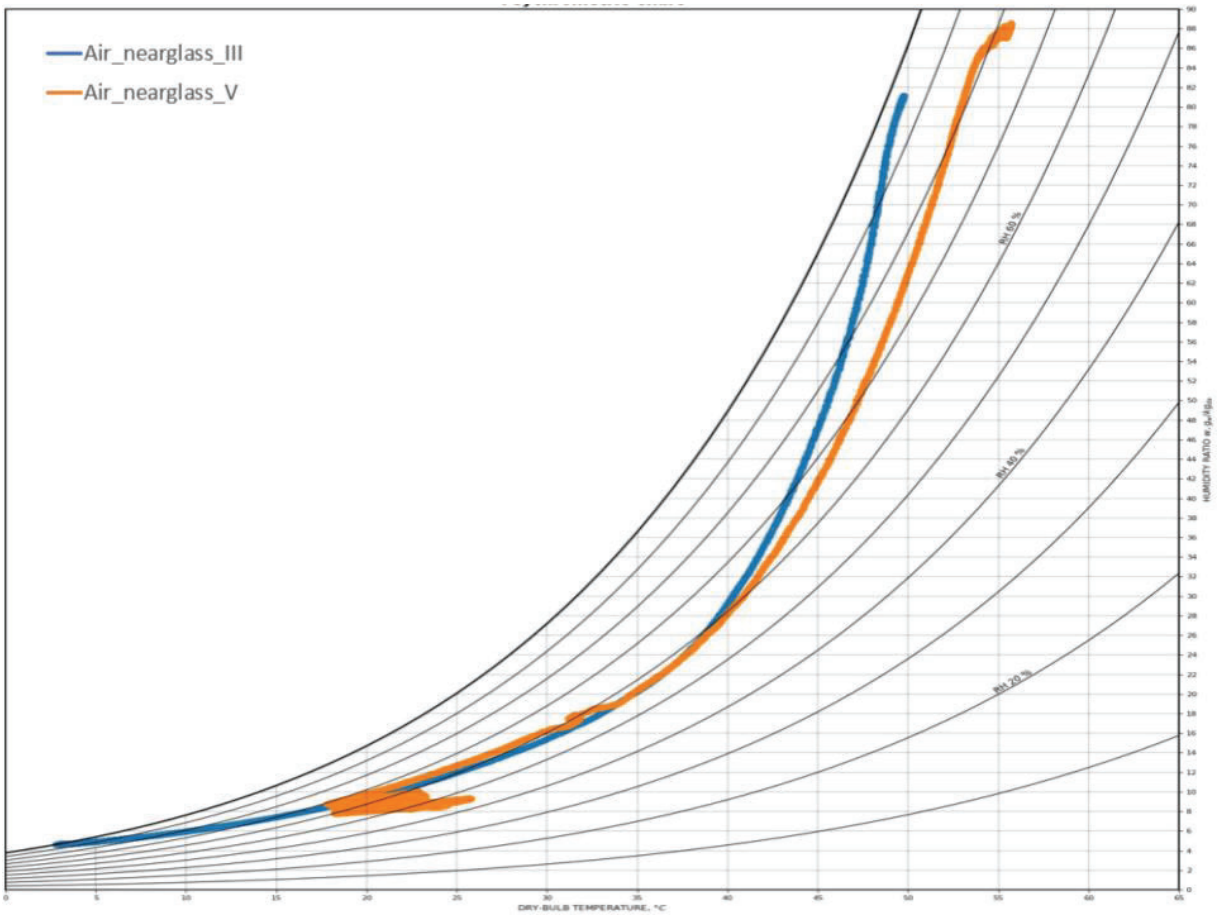

Figure 5.7: Psychrometric chart for all the tests with two sensors, showing the psychrometry of the air close to the glass cover

5.3 Tests with four sensors

In these tests, the pt100 temperature sensor was removed and replaced by another SHT85 as well as an addition of two more SHT85 sensors, in total four SHT85 sensors, in order to collect more comprehensive data.

Figure 5.8, 5.11, 5.13 and 5.15 shows the eight sensor values for tests XII, VII, XI and X. For a more detailed description of the tests see table 4.1. The temperatures are plotted in variants of blue and grey while the humidity curves are plotted in green, yellow, brown orange

The figures 5.9, 5.12, 5.14 and 5.16 plots the fog value for the tests, XII, VII, XI and X. These graphs show and compare the fog value for the sensor places close to the glass and the sensor placed in the middle of the camera. The orange curve illustrates the fog value of the sensor in the middle the camera while the blue curve illustrates the fog value of the sensor near the glass. Note that in these graphs, a fog value below zero indicates that fog has been formed. For example in test XII

is detected accurately while in test VII the test shows a false negative since fog is formed but not detected.

Figure 5.10 shows the temperature difference between the glass and close to the glass.
Figure 5.17 shows a psychrometric chart of the psychrometric movement of the air, close to the glass cover and the air in the middle of the camera for tests XII and XI, X, and VII, during a cooling process.

5.3.1 Tests where the camera is powered off

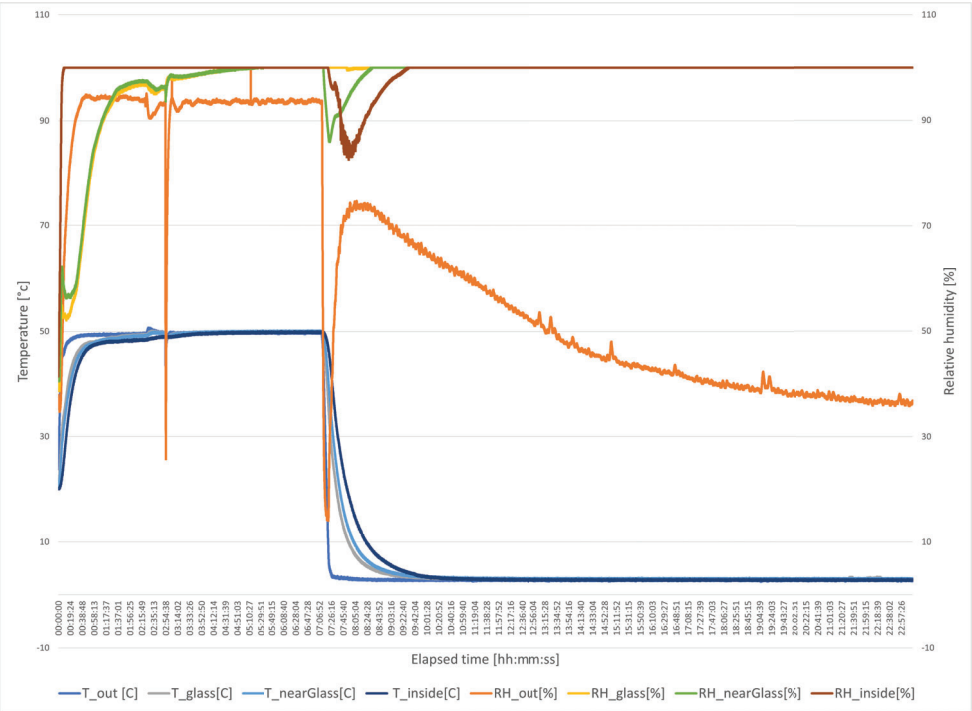

Figure 5.8: All the sensor inputs from test XII, the relative humidity and temperature from the four sensors.

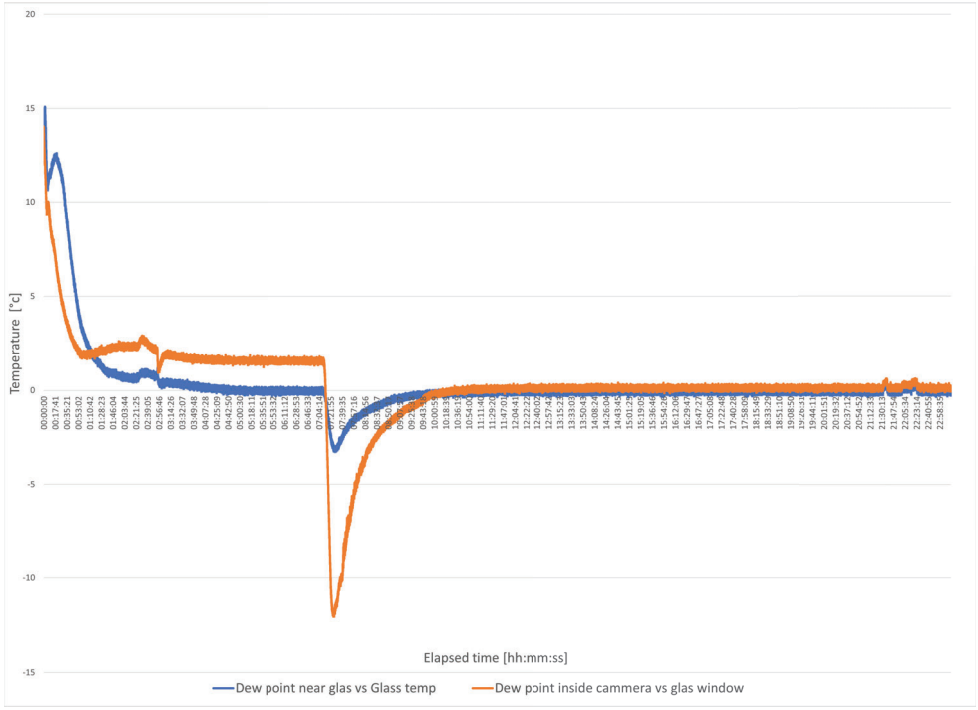

Figure 5.9: The difference between the glass temperature and the dew point for both the sensor near the glass and the sensor in the middle of the camera for test case XII.

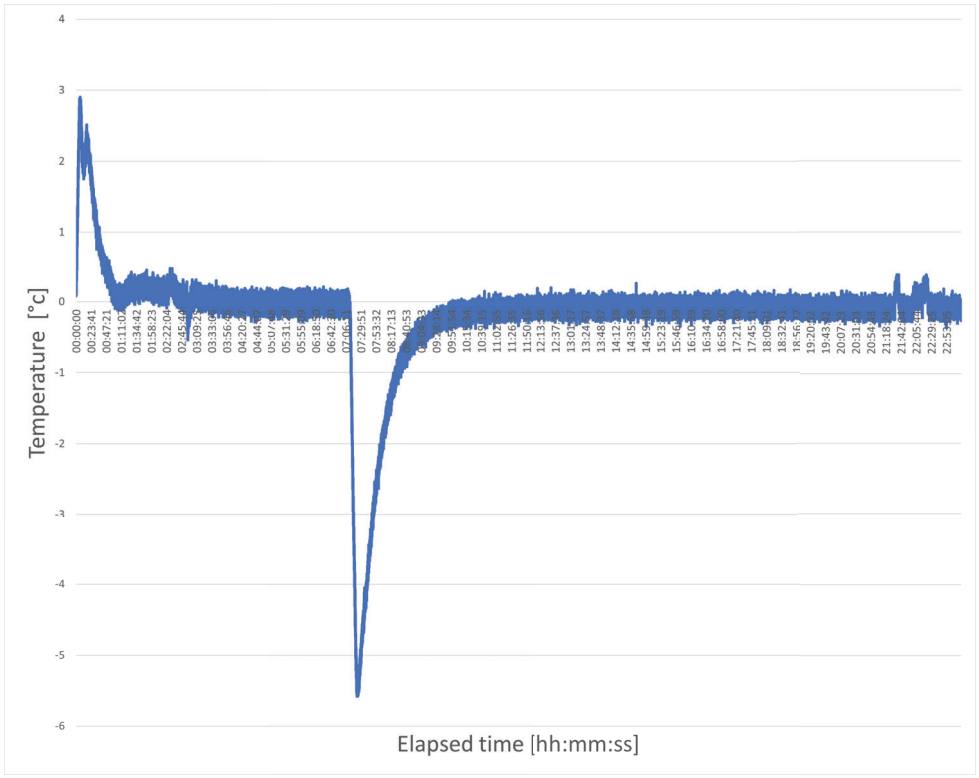

Figure 5.10: Shows the temperature difference between the glass and near the glass for test XII.

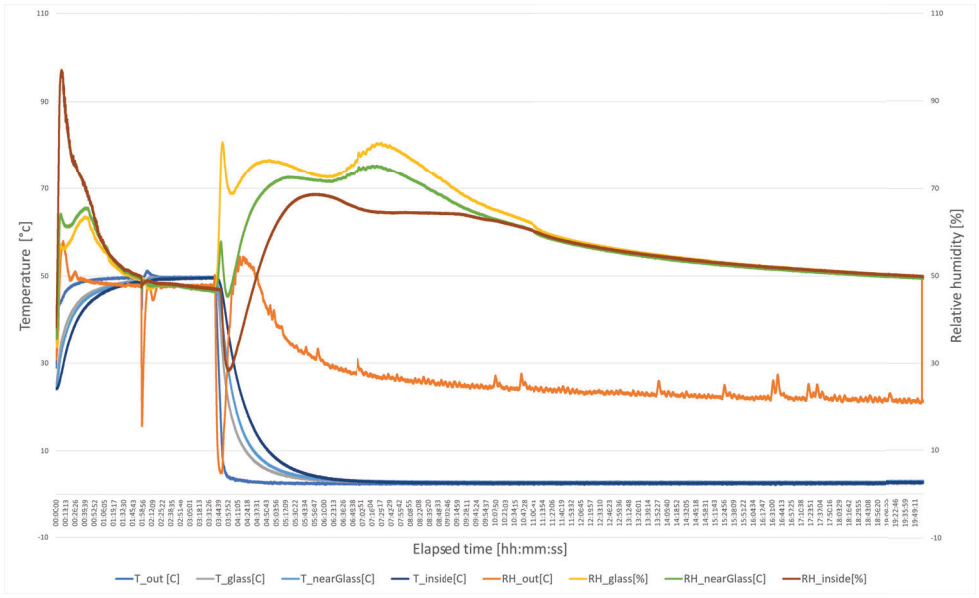

Figure 5.11: All the sensor inputs from test VII, the relative humidity and temperature from the four sensors.

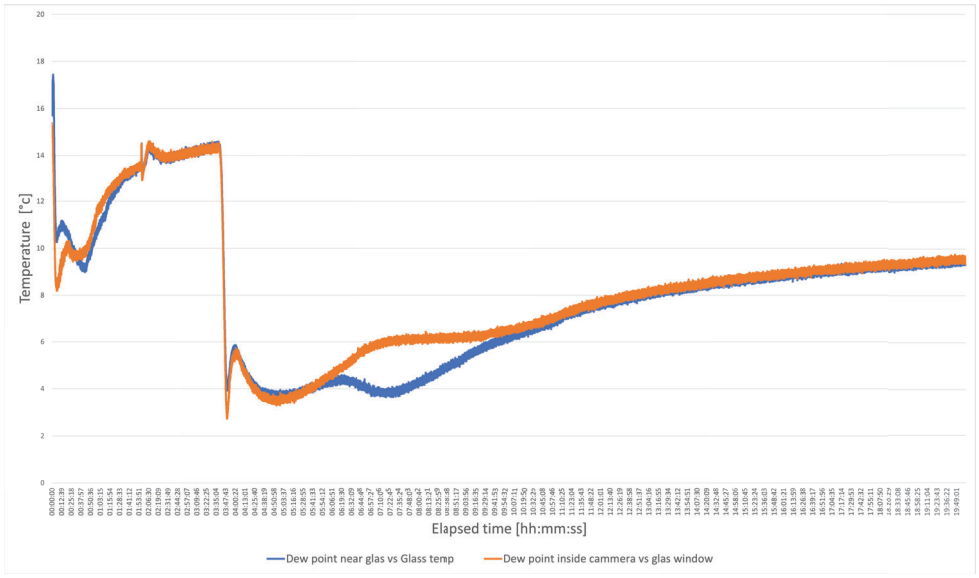

Figure 5.12: The difference between the glass temperature and the dew point for both the sensor near the glass and the sensor in the middle of the camera for test case VII.

5.3.2 Tests where the camera cover is slightly open

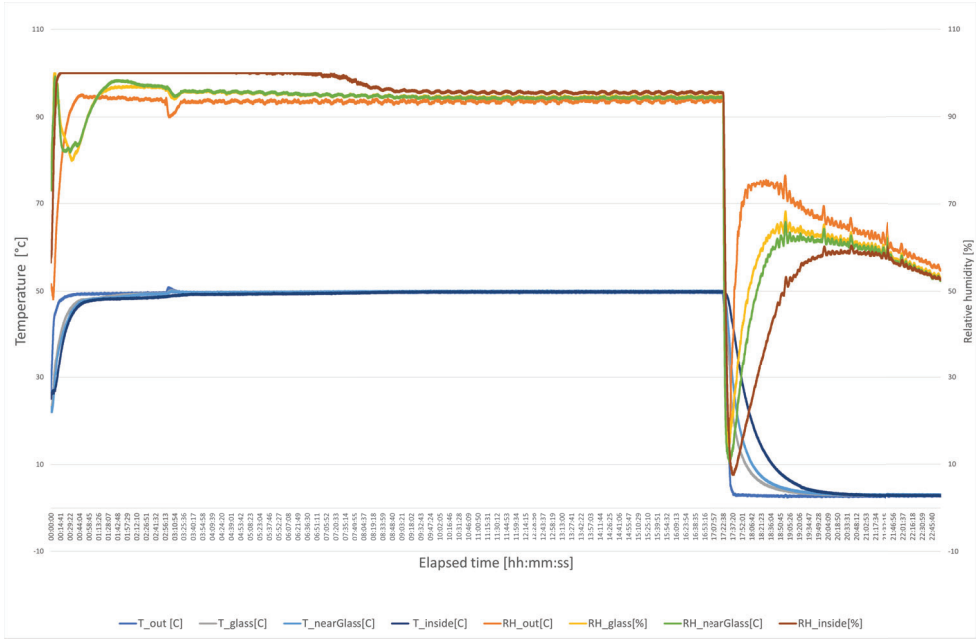

Figure 5.13: All the sensor inputs from test XI, the relative humidity and temperature from the four sensors.

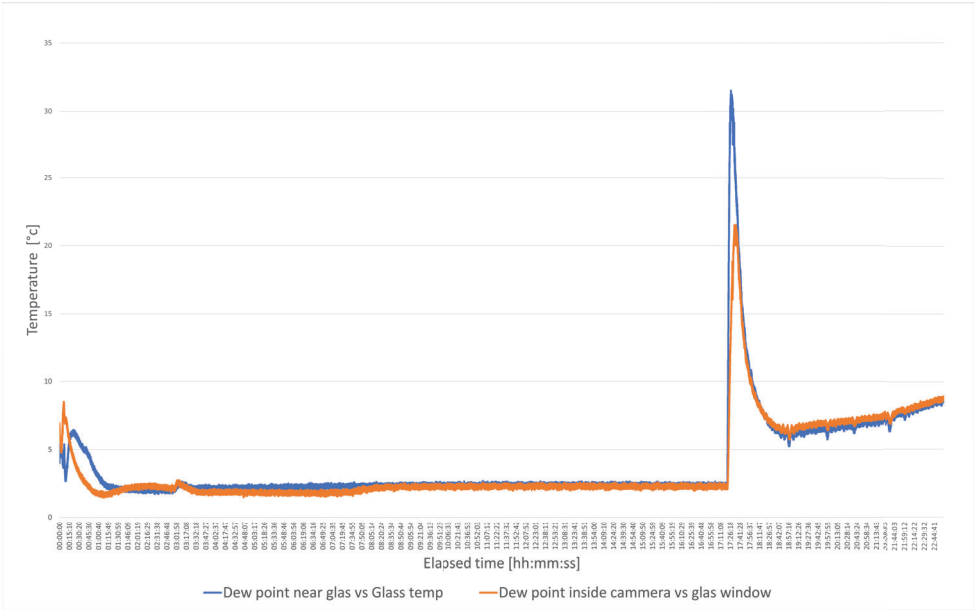

Figure 5.14: The difference between the glass temperature and the dew point temperature for both the sensor near the glass and the sensor in the middle of the camera for test case XI.

5.3.3 Tests where the camera heater is turned on manually

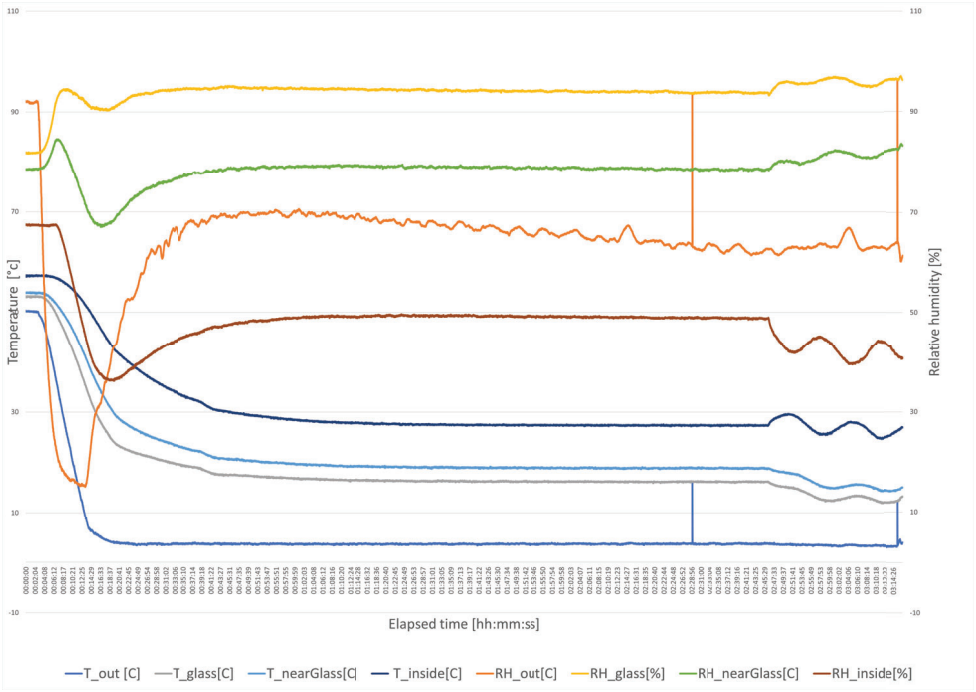

Figure 5.15: All the sensor inputs from test X, the relative humidity and temperature from the four sensors.

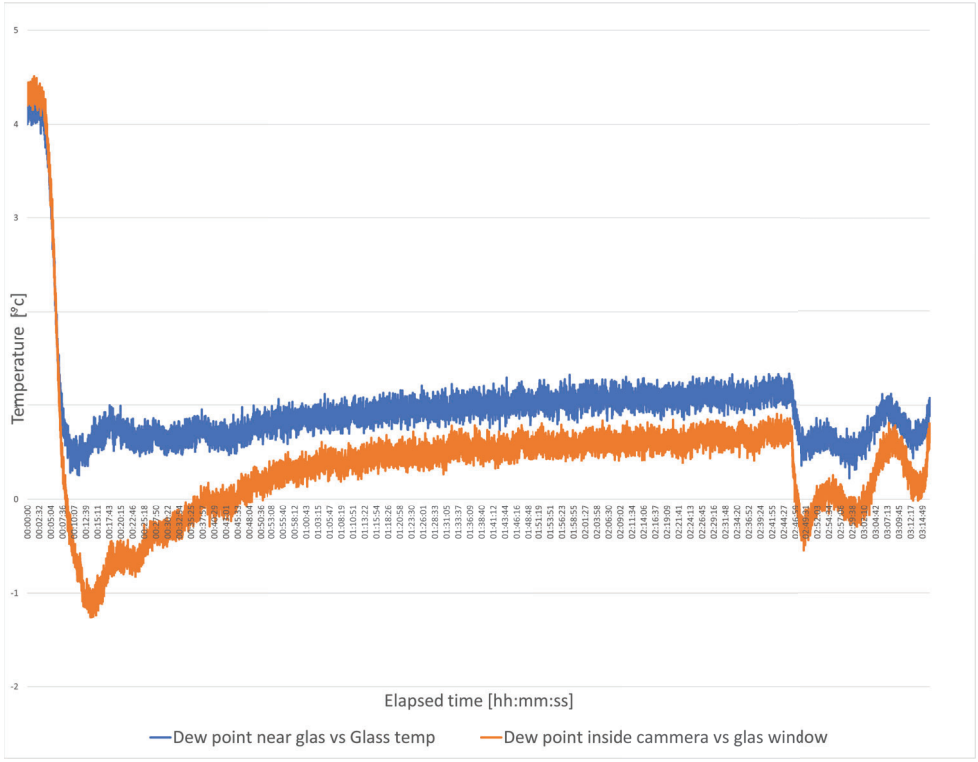

Figure 5.16: The difference between the glass temperature and the dew point temperature for both the sensor near the glass and the sensor in the middle of the camera for test case X.

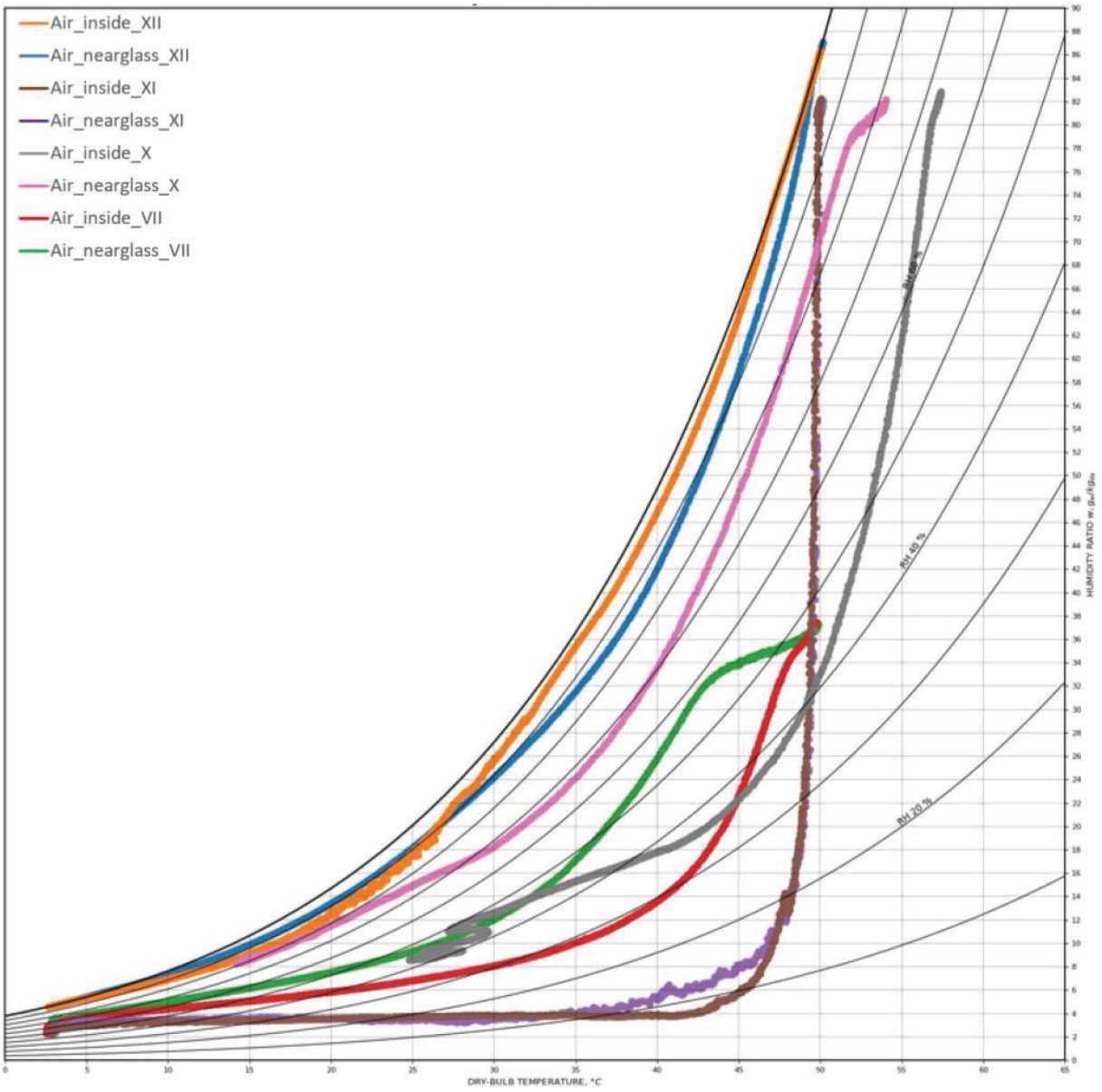

Figure 5.17: Psychrometric chart for all the tests with four sensors, showing the psychrometry of the air close to the glass cover and the air in the middle of the camera.

Chapter 6

Discussion

This chapter presents an interpretation of the results from the performed tests and critically evaluates the testing methodology, discusses the limitations encountered, and assesses the impact of these issues on the outcomes. Additionally, it identifies potential future research and enhancements to the existing model and finally a conclusion, addressing the success of the study.

6.1 Discussion and findings from the result

The Figures, 5.2,5.5,5.8,5.11,5.13,5.15, that displays all measured data from tests were added in order to provide an understanding of how the data change over time. From these graphs, trends are visualized for analytic purposes such as locating drops in humidity and temperature and at which rate.

The figures, 5.3,5.6,5.9, 5.12, 5.14, 5.16, display fog values over time, and can be used to interpret when fog is not detected.

The first set of figures is mainly included to provide an overall view of the conditions during the test and is used as a compliment to the later, and more important set of figures which displays fog value. From all figures, exact values may be difficult to extract. However, the overall trend is what is of significance rather than the exact value at the exact time.

Disclaimer

As a brief disclaimer, some explanations of the results that have been found in this thesis are still unknown. However, an attempt will be made to provide an explanation for certain interesting observations. The purpose of this is to present a potential solution or explanation based on observations and logic. Additionally, the addition of the presented solution may not be in accordance with the required standards for a commercial electronics product, however, as mentioned this study focuses on producing a proof of concept.

Analysing of the psychrometric chart

The psychrometric chart in figure 5.17 displays tests XII, XI, X and VII where some interesting observations are found. Test XII, XI and X are all run with the same external conditions, namely they start at temperature conditions T50°C RH90% $\rightarrow$ T3°C RH:Off, but various parameters are different. In test XII the camera is off and closed, in test X the camera is on, closed and has heaters and fans enabled while in test XI the camera is off but the lid is slightly open. These variations can be seen to produce significantly different psychrometric results and can be interpreted to indicate that both heating and ventilation have a positive effect on avoiding condensation. This is mainly derived from comparing the graphs with respect to how far each graph is from the saturation/dew point line. Moreover, it can also be concluded that this graph indicates that opening the camera yields the best result in fog reduction since it provides better moisture ventilation. This can be seen in the graph as the nearly vertical drop in absolute humidity, thus drastically reducing the dew point.

The representation of when condensation forms, illustrated by figure 2.4, shows a visualization of how the DPT can be extracted from a psychrometric chart, which is was is compared to the glass temperature in order to get the fog value. However, since the psychrometric charts do not give any sense of time, and the glass temperature could not be added in any meaningful way, it is inherently not possible to match the glass temperature with the corresponding psychrometric state of the air at a given time. Therefore, the psychrometric chart is not used to assess the risk of fog but instead provides other useful information, for instance how the temperature and humidity of a system move simultaneously and to compare tests.

Temperature controller

In test X when the internal camera heater is activated to control the temperature, the fog value of the curve in figure 5.16 undershot below zero even though no fog had formed. This is a false positive, but nonetheless, the camera might still have been at risk of fog. Since by studying figure 5.15, it is clear that the temperature difference between the glass and inside the camera, when the heater is on, is quite large.

Hence, it is worth considering if it would be beneficial to base the inside temperature on a temperature relative to the outside temperature and not a fixed value, to reduce the great temperature difference between the glass and inside air, causing an unnecessary big heat transfer, due to a large temperature gradient. The reduction of the temperature would mean that less heat would be transferred to the environment due to lower temperature potential. Another possible action is to consider if the heating could be done more evenly throughout the camera to reduce the difference between the air and the glass temperature.

Sensor placement

It is important to be careful when drawing conclusions from experimental data, as the outcomes can be anecdotal from the specific test being conducted. Although, as seen in the figures 5.9, 5.12,5.16, fog is detected more reliably when calculating the fog value based on the inside (the middle) of the camera compared to close to the glass.

These results regarding sensor placement were contradictory to the literature in the pre study. For instance, the literature from the automotive industry concluded that sensors should be placed close to the windshield in order to get the best fog detection results. Additionally, it was mentioned that the sensors should not be placed close to fans or heaters since that could affect the result. One possible explanation is that the middle of the camera could be a less chaotic environment, sheltered from internal air and temperature streams. A second possible explanation is that the air temperature near the glass is too heavily affected by the cooling from the window and thereby a poor representation of the air inside the camera. However, due to the big temperature gradients within the camera, even further investigating of optimal sensor placement is suggested in order to receive the most reliable detection results.

6.2 Evaluation

Unexpected behavior from the climate chamber

During testing, it was observed that the climate chamber decreased humidity before temperature when instructed to cool rapidly, regardless of what the humidity reference was set to. The behavior could be intentional since dehumidified air, which contains less water, has a lower heat capacitance than humid air, thus requiring less energy to cool the entire gas-vapor mixture. It could also be a precautionary step to prevent condensation in the chamber during cooling. A final potential reason could be that it is not intentional, but rather a consequence of condensation occurring at the cooling element which reduces the overall humidity in the system.

This behavior of the climate chamber invalidated test VIII which tried to evaluate how temperature and humidity would affect fogging amount inside the camera when only changing the temperature. Additionally, since the parameters of the climate chamber were kept similar for most tests, it is reasonable to assume that most tests, therefore, experienced this rapid drop in humidity. To which extent this influenced the results are unknown, but the fog was produced nonetheless.

Excessive moisture remaining from previous testing

Time was a factor in this project, hence different tests were conducted for several days in a row, to save some time. The goal of many tests was to generate fog inside the camera and occasionally

some condensate remained in the camera afterward. This remaining water after the test was attempted to be removed manually, but how successful the attempts were is unknown. Although all visible moisture was removed, some moisture may have been absorbed by the materials or hidden in unreachable spots inside the camera which could have influenced the moisture levels during the subsequent test.

An example where subsequent tests may have been affected by remaining moisture is when comparing the two almost identical tests III and XII. Comparing figures 5.8 and 5.2 shows significant differences in humidity which also can be seen when comparing the graphs from the tests in a psychrometric chart, seen in the figures5.17 and 5.7. This could, however, be due to other factors such as sensor placement, but assumed to be mainly due to remaining moisture.

Issues with the testing method

The temperature and humidity used in most tests have been somewhat exaggerated to the point where such conditions would rarely occur in the field. However, reproducing an accurate representation of fog conditions is difficult in a lab environment. One reason is that it requires a substantial amount of knowledge about climate trends but primarily due to the fact that the amount of different climate conditions an outdoor camera is exposed to is extremely large and it is practically impossible to recreate every scenario. This is the justifying reason for the constant start and end climate conditions trough out the majority of tests.

The choice to keep identical conditions allowed for the isolation of parameter change and general repeatability which is considered positive. However, the specific choice of 50°C 90% RH to 3°C is, in retrospect, a large change. A reduced change, thus a more realistic scenario, could potentially have produced higher quality results and further ensure that the fog detection will work as intended in real world applications. Therefore, this choice of conditions may have produced results where fog is detected, but only proven at extreme levels of fog. Secondly, the large amount of produced fog did often not evaporate fully once the test was completed. Therefore, the data logging did often not include the camera going from a state of fog to a state of completely dry and consequently did not validate that the used detection method is reliable in detecting when the fog is removed. The aspiration was to resolve this by changing the conditions or by recording the test for longer but this was not possible due to time constraints at this point in the study.

As an example of this, test XII and VII started with the same temperature but one was dropped from RH90% and the other from RH45%. Both tests produced fog, however at different levels, but fog was only detected at the higher humidity test and not detected at the lower humidity level. As far as evaluating the reliability of the fog detection method, this may not seem promising. However, analyzing the data from test VII where the fog was not detected, a large drop in fog value occurs which means it should be possible to detect with a more sophisticated detection algorithm than

simply checking if the fog value is below zero. This study has however focused on developing the detection method, rather than advanced automated data analysis.

Uncertainty in measurements and calculations

One challenge during this study was the inherent uncertainty and error associated with both calculations and sensor readings. The accepted error specified in the hygrometry sensor data sheet grew larger closer to the saturation region which was concerning since that is the area of interest in this study. Additionally, the formulas used to calculate dew point temperature are essential to detecting fog in the used method. Therefore, any uncertainty, especially the risk of compounding errors would directly influence the uncertainty of fog being detected.

Given constraints in time and budget, addressing or removing this inherent uncertainty directly was not feasible. Hence, a degree of skepticism was necessary when interpreting the results such as accepting measurements and calculations as approximations, and not as absolute truths.

Problems with measuring relative humidity

The hygrometry sensors used provide an output in relative humidity rather than absolute humidity. This can complicate analysis since relative humidity is dependent on humidity but also temperature, meaning that the relative humidity changes as the temperature changes. Therefore the absolute humidity was calculated afterward in order to get a more comprehensive analysis. The calculations performed were not required to be accurate in value, but only remove the temperature dependence, thus minimizing the requirement of formulas with low uncertainty. Another approach could be to purchase sensors that output values in absolute humidity, however, such sensors were difficult to find.

Unexpectedly high rate of humidity loss trough filters

Previous tests have been conducted at the company to measure the rate of moisture transportation through the installed filters. However, the previously measured rates may not have been applicable in this study because of the large and rapid amount of cooling and humidification during testing in this study. This invalidation is speculative but still considered since diffusion is dependent on concentration, meaning that the rate of transportation through permeable membranes is increased when the difference in vapor concentration is increased.
Furthermore, when the climate chamber cools down, there is a rapid drop in absolute humidity in the climate chamber. Since the effects of diffusion are affected by the difference in concentration, the rate of transportation will increase when the difference in water moisture inside and outside increases. Consequently, the rate of transfer is likely to increase, if not limited by the capacity of the filters. However, it is unclear to what extent this influences the rate of moisture transfer through the filters on the camera. Since, according to the previous test performed by the Quality Assurance team at the company, the rate at which water moisture in the air is transferred through the filters

is relatively slow and it takes several hours to equalize the moisture level inside the camera with the ambient when a drop in humidity occurs. The details of this can also be found in test I, see table 4.1 for a description of the test and table 5.1 for the results of the test.

Cooling process theory not matching reality

Due to the relatively small amount of air and low rate of moisture dissipation in the camera, it was at first assumed to represent the cooling process described in section 2.9. Hence it was expected that, when the camera was cooled down, the air in the camera would first cool down without change in absolute humidity until it reached the dew point and then later lose moisture to condensation. However, this has not been the case. By studying the psychrometric charts for the different tests that are shown in the results chapter in figure 5.7 and 5.17, the psychrometric charts do not resemble the expected standard cooling process represented by the dotted lines in figure 2.6. This difference may be due to two reasons, illustrated with two examples:

Imagine a cold soda beverage can be taken out of the fridge on a warm summer day and placed in a room. As noted from experience, there is a high risk that fog will form on the side of the can that contains the beverage. Furthermore, imagine a temperature sensor placed in this room at an unaffected distance from the beverage. If the temperature of the room is measured before the beverage was placed in the room and after the fog had formed on the can/bottle. It is unlikely that the bottle would have any noticeable effect on the temperature of the room, yet fog has still formed on the can.
Anecdotally, when a cold soda can gets covered in condensation at room temperature, the humidity and temperature in the room are not measurably reduced due to the comparably large air volume of the room. Measurements of room psychrometrics would therefore not show a standard HVAC cooling process. Similarly, the heat capacity and heat generation in the camera may be unproportionately large compared to the cooling from the glass, thus not mimicking the initially expected theoretical process which is described in section 2.9.

Another possible reason is due to underestimating the dissipation of water moisture from air from the filters.If the filter dissipation is higher than expected, a drop in humidity might not be a result of condensation, but rather moisture dissipating through the filters. Such dissipation is not included in the standard HVAC cooling process and may therefore be a reason for the unexpected results.

Background theory not matching reality

During the research of this thesis, there were some interesting details regarding our final concept that would have been very beneficial to achieve but that is something that we did not find during our testing to achieve.

During the pre study, some concepts seemed promising but proved to be implausible during testing.

For instance, one of the reports found that the humidity would remain at 100% humidity until all fog had evaporated. This was observed in some tests in this thesis study but not all. One example of where it was evident was in 5.8, while it was not shown in figure 5.11 nor in 5.15. In figure 5.15 it remains high even when most condensate is gone while in 5.11 it does not reach 100% even though fog is formed.

Another interesting observation from the theory, described in subsection 2.10.1, was that through the chosen method, fog should not only be possible to detect but also predict. However, whether this is true or not could not be determined for certain from the test performed. The humidity and temperature were reduced too rapidly to be able/have time to predict fog. Furthermore, the times at which the fog values undershot the value 0 corresponded quite well with when the fog was detected on the camera. Hence from this from this reasoning, the conclusion should not be drawn that it is not possible to predict reason using this concept, but rather that it was not proved in this study. Not being able to prove that it is possible to predict fog was somewhat disheartening, as it was one of the key appealing features that led to the selection of this particular method. However, it is also not proven that it is not possible to predict, leaving room for potential future work.

Limitations based on company desires

Besides time constraints and physical limitations, this thesis was occasionally limited by expectations and requirements from the collaborating company. One such requirement was to refrain from utilizing external sensors since it could reduce the water resistant properties of the product. This mainly influenced the study by disregarding frost detection as it almost exclusively occurs on the outside. However, not using external sensors may also influence fog detection capabilities since fog is primarily caused by external conditions, meaning that additional external data could have been useful.

6.3 Findings outside the scope

Analytical model for fog evaluation and prevention

Beyond the main focus of detecting fog, this study has also led to a new method for analyzing the air and moisture inside the camera. Although not initially part of the project's scope, this unexpected result holds significant potential value. The developed method has provided insights into how fog can be measured, but also key factors around conducting tests in the area of air and moisture such as sensors, timings, theoretical models, test conditions, common errors, calculations, methodology, software, analysis techniques and so on. This could be of great use for instance when developing prevention of fog, both by utilizing the insights from this study and also by using fog value and psychrometric as a metric when validating the effectiveness of said prevention technique.

Furthermore, by comparing the figures that show the fog value of tests X, XI and XII in figure 5.9, 5.16 and 5.14 or their psychrometric movement in the psychrometric chart (figure 5.17) there is a significant difference between their appearances. Hence this analytical tool can be used to evaluate which of the two removal methods that yield the best effect on the psychrometry of the air for avoiding condensation. By using the rule of thumb, the further away from the dew point line or the further away from the fog value of 0, the lower the risk is for condensation to form.

The subject of distinguishing between frost and fogging has not been investigated in great detail. However, some interesting observation on the subject has been made which can help to speed up future work within this field. Firstly the most obvious criterion for distinguishing between fog and frost is simply by measuring the freezing point. The phenomenon of fog and frost are quite similar on a macro scale, in the sense that both of them occur when water from the air condenses on a surface. If the freezing point is below zero degrees Celsius, frost will likely start to form.

Based on the pre study, if frost detection was chosen to be further evaluated in this study, the most promising methods would be by measuring capacitance on the outside of the glass or by an infrared sensor through the glass if restricted by not being able to mount sensors on the outside. Speculatively, frost could be detected using hygrometry as well, but to which extent this would be reliable is not known.

6.4 Future work

The work and results from this study have demonstrated great potential regarding fog detection by utilizing combined temperature and hygrometry sensors. However, the results from this study present a proof of concept rather than a refined solution and therefore some suggested future work is presented.

Tests that heavily rely on climate conditions are naturally time consuming, therefore more testing would be beneficial. Some examples of tests that would be recommended to perform are real world field testing, testing other temperatures, and humidity levels and at which rate they change, more advanced control of heaters and fans, other similar sensors, and testing on other cameras.

One topic in particular, which is outside the scope of this study, is refining the analytical model of the sensor data. The theories of psychrometry state that any air cooled below the dew point will begin to form a condensate. However, this became clear to not always be the case based on a number of factors and therefore, refining the software side of this study might greatly improve the results. A simple approach could be to calculate the probability of fog, rather than a binary output, whereas a more advanced approach could be to collect training data and develop a machine learning model to predict fog. The level of sophistication can vary, but nonetheless, there is room for improvement.

Furthermore, one of the main benefits of hygrometry was the potential to not only detect fog but prematurely predict fog. Besides a refined analytical model, more tests could be performed such as with a slower temperature change. This is because the tests in this study only tested rapid changes where there was not enough time to predict.

The created concept in this study can additionally be used to evaluate different removal/prevention methods, described further in the subsection 6.3. Meaning, the proposed solution in this study can, besides measuring and detecting fog, streamline the development of any chosen removal method. The goal is to maintain a lower glass temperature than the dew point temperature, which is not possible to do without influencing the psychrometry inside the camera.

Another way to elaborate on this study is to evaluate whether hygrometry could be used to detect frost or improve current approaches to detect frost. The reason why hygrometry may be able to detect frost, as well as fog, is because both fog and frost formation is primarily caused by airborne water adhering to a surface.

6.5 Conclusion

This project has demonstrated that it is possible to detect the presence of fog inside a surveillance camera by using a combined hygrometer and temperature sensor to calculate the dew point temperature of air and compare it to the glass temperature.

As mentioned in the scope and goal in section 1.2, the goal of this study was to "develop a proof of concept for an energy-efficient and reliable solution for detecting the presence of fog and frost". To which extent this was successful is concluded below.

Regarding energy efficiency, the energy consumption of the solution was never measured or compared to the discussed alternative solutions. The reason for this is mentioned in the introduction which is that the main goal is not to minimize the energy consumption of the sensor device but rather to improve the energy consumption of the camera. Meaning, the solution should consume an insignificant amount of energy compared to the energy savings it enables. For instance, being able to detect fog implies being able to remove unnecessary heating or be able to lower the overall temperature in the camera, which this solution has the potential to do.

The reliability of the solution is a more complicated topic. The actual detection results from the study were not greatly reliable, but this is based on that detection should be done automatically by the system. The cases where the fog was present but not detected automatically still showed drastic changes in fog value from the raw data and could easily be detected by a more advanced detection algorithm. Therefore, the reliability of the proof of concept may be low, but the potential reliability is regarded as very high.

As mentioned in the introductory section, frost became disregarded during the study, however, some findings in the area of frost detection were still found and could provide useful in future research.

In conclusion, a proof of concept to detect the presence of fogging on the protective glass/plastic cover on outdoor network cameras was successfully developed, the solution consumes an insignificant amount of energy compared to the potential energy savings from detecting fog, demonstrates a potential to be reliable and finally, holds significant promise as an effective detection method.

Bibliography

[1] KA Abbas, AM Saleh, O Lasekan, HA Abbas, et al. Significance and application of psychrometric chart in food processing: A review. *Journal of Food, Agriculture and. Environment*, 8:274–278, 2010.

[2] Sensorion AG. Sht85 digital pin-type humidity and temperature sensor [internet]. url: `https://sensirion.com/products/catalog/SHT85/`, 2023. cited 16-03-2023.

[3] ML Aguiar, PD Gaspar, and PD Silva. Frost measurement methods for demand defrost control systems: A review. In *Proceedings of the World Congress on Engineering*, volume 2, 2018.

[4] ML Aguiar, PD Gaspar, and PD Silva. Further development and experimental testing of a resistive sensor for monitoring frost formation in refrigeration systems. In *25th IIR International Congress of Refrigeration*. The 25th IIR International Congress of Refrigeration (ICR 2019), 2019.

[5] ML Aguiar, PD Gaspar, PD Silva, and D Duarte. Testing of a resistive sensor with fabric medium for monitoring frost formation in refrigeration systems. *Procedia Environmental Science, Engineering and Management*, pages 205–214, 2021.

[6] ML Aguiar, PD Gaspar, PD Silva, AP Silva, and AM Martinez. Medium materials for improving frost detection on a resistive sensor. *Energy Reports*, 6:263–269, 2020.

[7] YA Cengel and MA Boles. Gas-vapor mixtures and air-conditioning. *Thermodynamics and Engineering Approach, 8th ed.; McGraw Hill: New York, NY, USA*, pages 725–729, 2015.

[8] LI Davis Jr, GA Dage, and JD Hoeschele. Conditions for incipient windshield fogging and anti-fog strategy for automatic climate control. *SAE transactions*, pages 537–545, 2001.

[9] Fabian. E. Psychrometric chart use [internet]. url: `https://extension.psu.edu/psychrometric-chart-use`, 2021. cited 07-02-2023.

[10] National geographic. Condensation [internet]. url: `https://education.nationalgeographic.org/resource/condensation`. cited 27-01-2023.

[11] National geographic. Frost [internet]. url: `https://education.nationalgeographic.org/resource/frost`. cited 27-01-2023.

[12] M Graça, PD Gaspar, PD Silva, J Nunes, and LP Andrade. Monitoring device of ice formation in evaporator surface of refrigeration systems. *VI Ibero-American Refrigeration Sciences and Technologies*, 2016.

[13] Texas Instruments. Capacitive sensing basics [internet]. url: `https://software-dl.ti.com/msp430/msp430_public_sw/mcu/msp430/CapTIvate_Design_Center/latest/exports/docs/users_guide/html/CapTIvate_Technology_Guide_html/markdown/ch_basics.html`, 2020.

[14] T Islam. Design and fabrication of fringing field interdigital sensors for physical parameters measurement. *Interdigital Sensors: Progress over the Last Two Decades*, pages 71–90, 2021.

[15] MG Lawrence. The relationship between relative humidity and the dewpoint temperature in moist air: A simple conversion and applications. *Bulletin of the American Meteorological Society*, 86(2):225–234, 2005.

[16] M Marcelić and R Malarić. System for early condensation detection and prevention in residential buildings. In *2017 40th International Convention on Information and Communication Technology, Electronics and Microelectronics (MIPRO)*, pages 162–165. IEEE, 2017.

[17] M Mohsen-Nia, H Amiri, and B Jazi. Dielectric constants of water, methanol, ethanol, butanol and acetone: measurement and computational study. *Journal of Solution Chemistry*, 39:701–708, 2010.

[18] AR Peters. Interior window fogging-an analysis of the parameters involved. *SAE transactions*, pages 1720–1731, 1972.

[19] AR Petre, R Craciunescu, and O Fratu. Design, implementation and simulation of a fringing field capacitive humidity sensor. *Sensors*, 20(19):5644, 2020.

[20] P Singh. Relative humidity calculator [internet]. url: `https://www.omnicalculator.com/physics/relative-humidity.`, 2023.

[21] F Tartarini. Draw a psychrometric chart with python [internet]. url: `https://www.youtube.com/watch?v=AOwWZliweM8&t=1566s`, 2021. cited 12-04-2023.

[22] TM Urbank, SM Kelly, TO King, and CA Archibald. Development and application of an integrated dew point and glass temperature sensor. *SAE transactions*, pages 546–556, 2001.

[23] M Wang, TM Urbank, and KV Sangwan. "clear vision" automatic windshield defogging system. *SAE transactions*, pages 939–947, 2004.

[24] J Zhu, Y Sun, W Wang, Y Ge, L Li, and J Liu. A novel temperature–humidity–time defrosting control method based on a frosting map for air-source heat pumps. *International Journal of Refrigeration*, 54:45–54, 2015.

Appendix A

Code for measuring temperature and humidity with an arduino

This code is an Arduino sketch that reads temperature and humidity data from four SHT85 sensors and prints the data to a serial output. The sensors are read individually using an I2C multiplexer. The I2C multiplexer allows the Arduino to communicate with multiple sensors using a single set of I2C pins. An I2C bus could not be used because the SHT85 all have the same non-changeable default address.

The setup() function initializes all the necessary objects and features used in the sketch. Then the loop() function loops through each of the four sensors and reads the temperature and humidity data using the readAndPrintSHT() function. The setMuxPort() function is used to select the appropriate sensor for reading. The temperature and humidity data are then printed to the serial port.

During testing, the sketch is executed on an Arduino, and the serial output is read by a personal computer. The data is stored in a text file for later use.

```
1  //  FILE: SHT sensor array.ino
2  //  AUTHOR: Emil Hermansson & Viktor Hansson
3  //
4  //  TOPVIEW SHT85  ( SHT85 datasheet)
5  //            +-------+
6  // +-----\    | SDA 4 -----
7  // | +-+  ----+ GND 3 -----
8  // | +-+  ----+ +5V 2 -----
9  // +-----/    | SCL 1 -----
10 //            +-------+
11
12 #define SHT85_ADDRESS         0x44
13 #define number_of_sensors     4
14
```

```
#include "SHT85.h"
#include <SparkFun_I2C_Mux_Arduino_Library.h>

QWIICMUX myMux;
SHT85 sht;
int Sensor_pins[] = {0,1,5,7};

void setup() {
  Serial.begin(115200);
  Wire.begin();
  sht.begin(SHT85_ADDRESS);
  delay(1000);
  Serial.println("STARTING...");
  init_Mux();
  setMuxPort(0);
  //Wire.setClock(100000);
}

void loop(){
  Serial.print(String(millis() * 0.001, 0)); // time in seconds
  for(int sensorNumber = 0; sensorNumber < number_of_sensors; sensorNumber++){
    setMuxPort(Sensor_pins[sensorNumber]);
    Serial.print("\t");
    readAndPrintSHT();
    delay(3); //milliseconds
  }

  Serial.print("\n");
  delay(990); //milliseconds
}

void readAndPrintSHT(){
  sht.read();         // default = true/fast       slow = false
  float temperature = sht.getTemperature();
  float humidity = sht.getHumidity();
  Serial.print("," + String(temperature));  // SHT85 temperature
  Serial.print("," + String(humidity));     // SHT85 humidity
  return;
}

void init_Mux(){
  if (myMux.begin() == false)
  {
    Serial.println("Mux not detected. Freezing...");
    while (1){
      delay(2000);
      Serial.println("error");
    }
  }
```

```
64    Serial.println("Mux detected");
65
66    return;
67  }
68
69  void setMuxPort(int portNumber){
70    myMux.setPort(portNumber); //Connect master to port labeled '1' on the mux
71    //byte currentPortNumber = myMux.getPort();
72    //Serial.print("CurrentPort: ");
73    //Serial.println(currentPortNumber);
74    return;
75  }
76  // -- END OF FILE --
```

Appendix B

Code for transferring the raw measured data into a spreadsheet

This code transfers the raw data collected during the tests and transforms it into a spreadsheet. The code was created with the intention to simplify the simple logging of the data during the test, to allow for more structured processing of the data afterward.

The code can simply be compiled and run with any terminal, given that Python is properly installed. It only required the name of the script file, the name of the text file with the raw data, and the name on which the spreadsheet should be saved. However, this assumes that the data has been collected using the format used in appendix A. Observe that some file locations in the code have to be changed in order to work on other computers, this is done by changing the name of the file path on line 5.

```
1  import os
2  import math
3
4  # Get path to the folder containing the log files
5  folder_path = r"C:\Users\viktorha\Downloads"
6
7  # Prompt the user to enter the name of the file they want to convert
8  filename = input("Enter the name of the file you want to convert (without the .txt
       extension): ")
9  #filename="loggFromNight"
10
11 # Construct the full path to the file
12 file_path = os.path.join(folder_path, f"{filename}.log")
13
14 # Check if the file exists
15 if not os.path.isfile(file_path):
16     print(f"Error: File '{filename}.txt' not found in folder '{folder_path}'.")
17     exit()
18
```

```
# Prompt the user to enter the name of the output CSV file
output_filename = input("Enter the name of the output CSV file (without the .csv extension): ")

# Construct the full path to the output file
output_path = os.path.join(folder_path, f"{output_filename}.csv")

# Read the contents of the input file and convert it to a list of lines
with open(file_path, "r") as file:
    lines = file.readlines()

# Process the lines to extract temperature, humidity, and time data and write to the output file
with open(output_path, "w") as file:
    # Write the headers to the output file
    file.write("Time[s];T_out[C];RH_out[C];T_glass[%];RH_glass[C];T_nearGlass[%]; RH_nearGlass[C]; T_inside[C];RH_inside[%]\n")

    # Iterate over the lines and extract temperature, humidity, and time data
    for line in lines:
        # Ignore lines that contain non-numeric characters
        if not all(c.isdigit() or c in ".,-" for c in line.strip()):
            continue

        # Split the line into temperature, humidity, and time values
        try:
            stripped_line = line.strip(" \n")
            time, T_out, RH_out, T_glass, RH_glass, T_nglass, RH_nglass, T_inside, RH_inside = stripped_line.split(",")
            time = float(time)
            T_out = float(T_out)
            RH_out = float(RH_out)
            T_glass = float(T_glass)
            RH_glass = float(RH_glass)
            T_nglass = float(T_nglass)
            RH_nglass = float(RH_nglass)
            T_inside= float(T_inside)
            RH_inside = float(RH_inside)
            # Ignore lines that don't contain the expected number of values
        except ValueError:
            continue

        # Write the values to the output file with commas as the separator
        file.write(f"{time};{T_out};{RH_out};{T_glass};{RH_glass};{T_nglass};{RH_nglass};{T_inside};{RH_inside}\n")

print(f"Conversion complete. CSV file saved as '{output_filename}.csv' in folder '{folder_path}'.")
```

Appendix C

Code for plotting a psychrometric chart

This code plots a psychrometric chart and draws the lines of the states of the air during a cooling process based on the measured temperature and humidity.

The code is divided into two parts, first, the psychrometric chart is drawn. Then the lines describing the air's psychrometry are drawn. In this particular application, 10 lines are drawn for the different tests.

Most of the code was inspired by code found in reference [21]. However, the code was modified to fit this particular application. The code uses the libraries psychrolib and psychrochart which are useful for calculating and plotting the psychrometry of air.

The code can simply be compiled and run with any terminal, given that Python is properly installed. It only required the name of which the output picture should be saved with. However, Observe that some file locations in the code have to be changed in order to work on other computers. This is done by changing the name of the file path to a file path of where the file should be saved and including the name and type of the file that the file should be saved with, on lines 161 and 162.

```
1  ### Part 1
2  import matplotlib.pyplot as plt
3  import numpy as np
4  from psychrochart import PsychroChart
5
6  # Plots the Psychrometric chart
7  # Pass a dict with the changes wanted:
8  custom_style = {
9      "figure": {
10         # "title": "Psychrometric Chart (sea level)",
11         "x_label": "DRY-BULB TEMPERATURE, $ C$",
12         "y_label": "HUMIDITY RATIO $w, g_w / kg_{da}$",
```

```
        "x_axis": {"color": [0.0, 0.0, 0.0], "linewidth": 1.5, "linestyle": "-"},
        "x_axis_labels": {"color": [0.0, 0.0, 0.0], "fontsize": 8},
        # "x_axis_ticks": {"direction": "out", "color": [0.0, 0.0, 0.0]},
        "y_axis": {"color": [0.0, 0.0, 0.0], "linewidth": 1.5, "linestyle": "-"},
        "y_axis_labels": {"color": [0.0, 0.0, 0.0], "fontsize": 8},
        "y_axis_ticks": {"direction": "out", "color": [0.0, 0.0, 0.0]},
        "partial_axis": False,
        "position": [0.025, 0.075, 0.925, 0.875]
        },
    "limits": {
        "range_temp_c": [0, 65],
        "range_humidity_g_kg": [0, 90],
        "altitude_m": 0,
        "step_temp": 1.0
        },
    "saturation": {"color": [0.0, 0.0, 0.0], "linewidth": 2, "linestyle": "-"},
    "constant_rh": {"color": [0.0, 0.0, 0.0], "linewidth": 1, "linestyle": "-"},
    "constant_v": {"color": [0.0, 0.0, 0.0], "linewidth": 0.5, "linestyle": "-"},
    "constant_h": {"color": [0, 0.0, 0.0], "linewidth": 0.75, "linestyle": "-"},
    "constant_wet_temp": {"color": [0.0, 0.0, 0.0], "linewidth": 1, "linestyle": "
        --"},
    "constant_dry_temp": {"color": [0.0, 0.0, 0.0], "linewidth": 0.25, "linestyle"
        : "-"},
    "constant_humidity": {"color": [0.0, 0.0, 0.0], "linewidth": 0.25, "linestyle"
        : "-"},
    "chart_params": {
        "with_constant_rh": True,
        "constant_rh_curves": [10,20, 30, 40, 50, 60, 70, 80, 90],
        "constant_rh_labels": [20, 40, 60, 80],
        "with_constant_v": False,
        "constant_v_labels": [0.8, 0.85, 0.9, 0.95, 1.00, 1.05],
        "constant_v_step": 0.05,
        "range_vol_m3_kg": [0.8, 1.2],
        "with_constant_h": False,
        "constant_h_step": 50,
        "constant_h_labels": [50, 100, 150, 200, 250 ],
        "range_h": [0, 400],
        "with_constant_wet_temp": False,
        "constant_wet_temp_step": 10,
        "range_wet_temp": [-10,60],
        "constant_wet_temp_labels": [0, 10, 20, 30,40,50],
        "with_constant_dry_temp": True,
        "constant_temp_step": 5,
        "with_constant_humidity": True,
        "constant_humid_step": 2,

        "with_zones": False
        }
    }
```

```
59
60 fig, ax = plt.subplots(figsize=(20, 20))
61 chart = PsychroChart(custom_style)
62 chart.plot(ax)
63
64 # chart.plot_legend(markerscale=.7, frameon=False, fontsize=10, labelspacing=1.2)
65 #
    ----------------------------------------------------------------------------------

66 ### Part 2
67 import pandas as pd
68 import psychrolib
69
70 #Plots the lines in the psychrometric chart
71 #Change the address from where the file are read.
72 df = pd.read_csv(r"C:\Users\viktorha\Documents\Psychometric chart\24042023
       T50RHum90%with4sensorXII.csv", sep=";")
73 pressure = 101325
74 hr = []
75 for ix, row in df.iterrows():
76     hr.append(
77         psychrolib.GetHumRatioFromRelHum(row["T_nearGlass[C]"], row["RH_nearGlass
               [%]"]/100 , pressure)*1000 )
78 df["AH"] = hr
79 plt.scatter(x=df["T_nearGlass[C]"], y=df["AH"] )
80
81
82 hr2 = []
83 for ix, row in df.iterrows():
84     hr2.append(
85         psychrolib.GetHumRatioFromRelHum(row["T_inside[C]"], row["RH_inside[%]"
               ]/100 , pressure)*1000 )
86 df["AH2"] = hr2
87 plt.scatter(x=df["T_inside[C]"], y=df["AH2"])
88
89 df = pd.read_csv(r"C:\Users\viktorha\Documents\Psychometric chart\17042023T50RH45
       VII.csv", sep=";")
90 pressure = 101325
91 hr = []
92 for ix, row in df.iterrows():
93     hr.append(
94         psychrolib.GetHumRatioFromRelHum(row["T_nearGlass[C]"], row["RH_nearGlass
               [%]"]/100 , pressure)*1000 )
95 df["AH"] = hr
96 plt.scatter(x=df["T_nearGlass[C]"], y=df["AH"] )
97
98
99 hr2 = []
100 for ix, row in df.iterrows():
```

```
    hr2.append(
        psychrolib.GetHumRatioFromRelHum(row["T_inside[C]"], row["RH_inside[%]"
            ]/100 , pressure)*1000 )
df["AH2"] = hr2
plt.scatter(x=df["T_inside[C]"], y=df["AH2"])

df = pd.read_csv(r"C:\Users\viktorha\Documents\Psychometric chart\20042023
    T50H90toT3H0withOpenLidXI.csv", sep=";")
pressure = 101325
hr = []
for ix, row in df.iterrows():
    hr.append(
        psychrolib.GetHumRatioFromRelHum(row["T_nearGlass[C]"], row["RH_nearGlass
            [%]"]/100 , pressure)*1000 )
df["AH"] = hr
plt.scatter(x=df["T_nearGlass[C]"], y=df["AH"] )


hr2 = []
for ix, row in df.iterrows():
    hr2.append(
        psychrolib.GetHumRatioFromRelHum(row["T_inside[C]"], row["RH_inside[%]"
            ]/100 , pressure)*1000 )
df["AH2"] = hr2
plt.scatter(x=df["T_inside[C]"], y=df["AH2"])


df = pd.read_csv(r"C:\Users\viktorha\Documents\Psychometric chart\20042023
    HeaterMaxedduringcoolinX.csv", sep=";")
pressure = 101325
hr = []
for ix, row in df.iterrows():
    hr.append(
        psychrolib.GetHumRatioFromRelHum(row["T_nearGlass[C]"], row["RH_nearGlass
            [%]"]/100 , pressure)*1000 )
df["AH"] = hr
plt.scatter(x=df["T_nearGlass[C]"], y=df["AH"] )


hr2 = []
for ix, row in df.iterrows():
    hr2.append(
        psychrolib.GetHumRatioFromRelHum(row["T_inside[C]"], row["RH_inside[%]"
            ]/100 , pressure)*1000 )
df["AH2"] = hr2
plt.scatter(x=df["T_inside[C]"], y=df["AH2"])

df = pd.read_csv(r"C:\Users\viktorha\Documents\Psychometric chart\CameraOff III.
    csv", sep=";")
```

```
142 pressure = 101325
143 hr = []
144 for ix, row in df.iterrows():
145     hr.append(
146         psychrolib.GetHumRatioFromRelHum(row["T_nearGlass[C]"], row["RH_nearGlass
                [%]"]/100 , pressure)*1000 )
147 df["AH"] = hr
148 plt.scatter(x=df["T_nearGlass[C]"], y=df["AH"] )
149
150 df = pd.read_csv(r"C:\Users\viktorha\Documents\Psychometric chart\CameraOn V.csv",
      sep=";")
151 pressure = 101325
152 hr = []
153 for ix, row in df.iterrows():
154     hr.append(
155         psychrolib.GetHumRatioFromRelHum(row["T_nearGlass[C]"], row["RH_nearGlass
                [%]"]/100 , pressure)*1000 )
156 df["AH"] = hr
157 plt.scatter(x=df["T_nearGlass[C]"], y=df["AH"])
158
159
160
161 plt.savefig(r"C:\Users\viktorha\Documents\Psychometric chart\
    PsychrometricChart4sensors.jpeg", transparent=True)
162 plt.savefig(r"C:\Users\viktorha\Documents\Psychometric chart\
    PsychrometricChart2sensors.jpeg", transparent=True)
```